DYNAMICS OF A STRATIFIED TIN / WATER VAPOR EXPLOSION IN A CYLINDRICAL GEOMETRY

Thesis by Barbara Bruckert

Dept. of Mechanical Engineering
McGill University, Montreal
July, 1993

A Thesis submitted to the

Faculty of Graduate Studies and Research
in partial fulfillment of the requirements
for the degree of

Masters in Engineering

ABBREVIATED THESIS TITLE:

Dynamics of a Vapor Explosion in a Cylindrical Geometry

Dynamics of a Vapor Explosion in a Cylindrical Geometry

ABSTRACT

Recent studies have shown that the propagation of a vapor explosion in a stratified geometry is sustained, provided the degree of inertial confinement is sufficiently high. In the present study, the influence of boundary conditions on the propagation of a vapor explosion in a stratified tin/water system has been investigated experimentally. In one of two experiments, a propagating interaction was initiated, by an exploding wire triggger, in a channel formed by two sections of 1.25 cm and 5 cm in width. The interaction failed consistently at the transition into the larger channel, due to the sudden lateral expansion. The behavior of the interaction was also investigated in the absence of confining walls, accomplished by triggering it in the center of a cylindrical tank (27.30 cm in diameter; 4 kg of tin). The system's response to the trigger varied erratically: in just over half the cases an energetic interaction occured, while the initiation of an interaction failed in the other attempts. Successfully triggered interactions travelled radially outward, about 5 -11 cm from the center, at 30 - 60 m/s, producing overpressures of 0.15 to 0.5 MPa. The tin debris analysis indicated that only a thin layer of tin, ~.86 mm deep, was involved in the interaction. This event is, however, suspected to be the result of an overdriven interaction, rather than a sustained propagation. The inherent difficulty in initiating a propagating interaction in the cylindrical geometry lies in the effect of the divergence of the flow. The energy yield/surface area of the event is of the same order of magnitude as that of single tin drop/water explosions and stratified tin/water interactions in a narrow channel, suggesting that the energetics are not significantly influenced by the geometry. This interaction, in many cases, served as a "precursor" event for a second, more energetic interaction, initiated in the coarse mixture of water and molten tin fragments lofted in the wake of the first interaction.

RESUME

Les études récentes ont montré que la propagation d'une explosion de vapeur, en milieu stratifié, est autonome, sous réserve que le degré de confinement est suffisamment important. Dans la première phase de cette étude, l'influence des conditions aux limites sur ce type de propagation a été expérimentalement observé plus particulièrement pour une couche d'étain immergée dans de l'eau. L'explosion, initiée à l'aide d'un fil explosé, se propageait dans un réservoir de forme allongée, comportant deux sections de largeur de 1.5 cm puis 5 cm. L'expansion brutale, due au changement de section, conduisait, à chaque fois, à l'amortissement de l'explosion. Dans la seconde partie de l'étude, les effets de l'absence de confinement par les murs ont été aussi étudiés en amorçant l'explosion de vapeur au centre d'un réservoir cylindrique ($\phi = 27.3$ cm, 4 kg d'étain). Le comportement de l'initiation de la propagation était très erratique : dans environ la moitié des cas, une violente explosion fut observée, tandis que dans le reste des cas, la propagation ne s'amorçait pas. Lors de l'amorçage réussie, la propagation se déplaçait radialement, sur une distance de 5 à 11 cm, à une vitesse de 30 à 60 m/s, et accompagnée d'une surpression de l'ordre de 0.15 à .5 MPa. Cependant, ce mode de propagation est probablement le résultat d'une interaction surpoussée, plutôt qu'autonome. L'analyse des débris d'étain a montré que seule une couche mince d'étain, de l'ordre de 0.86 mm, contribue réellement à l'explosion. La difficulté inhérente à l'amorçage de la propagation de l'explosion en milieu non confiné est due à la divergence de l'écoulement. Le rapport densité d'énergie sur surface d'interaction étain/eau est du même ordre de grandeur que celui d'une gouttelette d'étain dans l'eau, ou que celui d'une explosion stratifiée étain/eau dans un canal étroit. Ce résultat suggère donc que l'énergétique n'est pas influencé de manière significative par la géométrie. Dans de nombreux cas, ce mode d'interaction servait de précurseur à une seconde explosion, beaucoup plus énergétique, déclenchée dans le nuage de fragments d'étain, en suspension dans l'eau, généré par le passage de la première explosion.

ACKNOWLEDGEMENTS

This work was not accomplished without the influence and company of a few individuals whom I would particularly like to mention.

Firstly, I would like to thank my supervisor, Prof. David Frost, for his guidance and understanding during the course of this work, and especially for his constant ability to provide a clear-sighted perspective of matters. I have also benefited from many stimulating discussions with Prof. John Lee, who is never short of ideas and suggestions, nor desire to share them. I have appreciated his enthusiasm, both in and out of school. I am grateful to Dr. Olivier Peraldi for his willingness to offer technical assistance and suggestions during the ealier stages of the experiments. Gaby Ciccarelli's phantom still lurks in the steam explosions lab; I am grateful for his shared interest and suggestions toward this study, as well as his valuable editorial assistance. Without too many words, I have enjoyed working nearby my friends Julian and Aris, and have appreciated our many constructive discussions. Finally, I would like to thank the Mech. Lab. II and Summer students: Karim, Dwayne and David, for their participation in the experimental work.

This research was sponsored by the National Sciences and Engineering Research Council of Canada.

TABLE OF CONTENTS

		Page	no.
Abstract		i	i
Resume		iii	
Acknowledgments		iv	
Tab	le of contents	•	/
List	of figures / tables	,	vii
Non	nenclature	i	X
1.0	Introduction		1
	 1.1 Spontaneous nucleation theory 1.2 Vapor film stability and triggering 1.3 Fragmentation and mixing 1.4 Propagation 1.5 Objectives and outline of present study 	1	3 4 8 10 18
2.0	Experimental facility and instrumentation	1	9
3.0	Results	2	21
4.0	 3.1 Initial conditions 3.2 Characteristics of the interaction 3.3 Features of the initiation stage of the interaction 3.4 Perturbation of the initiation front 	2	21 21 24 25
4.0	Discussion	2	27
	 4.1 Highly confined propagation in a narrow channel 4.1.1 Characteristic features of the propagating interaction 4.1.2 Energetics of the interaction 4.1.3 Pressure field in the water using a potential flow model 4.1.4 Effect if inertial constraint 4.2 One - dimensional vapor expansion model 4.2.1 Model description 4.2.2 Results of the effect of inertial constraint 4.3 Perturbation of the interaction front 4.4 Effect of the unconfined condition in the cylinder on the interaction characteristics 	22 23 33 33 33 33 33	27 28 29 30 30 31 32 33

4.4.1 Initiation of the interaction 4.4.2 Energetics	34 37		
5.0 Conclusions	39		
Figures			
References			
Appendix A			
Appendix B			

LIST OF FIGURES AND TABLES

- Fig.1 Illustration of spontaneous nucleation model.
- Fig.2 Boiling curve for water.
- Fig.3 Fuel-coolant interaction zone for 1.2 x 10⁻² kg of tin dropped into water.
- Fig.4 Pressure impulse for various water heights in narrow channel.
- Fig.5 Schematic of Harlow and Ruppel vapor explosion propagation model.
- Fig.6 Schematic of experimental facility.
- Fig.7 Schematic of cylindrical tank.
- Fig.8 Illustration of the growth of the first interaction in the cylindrical geometry.
- Fig.9 Pressure recorded during single interaction in cylindrical tank.
- Fig. 10 Distribution of tin fragment sizes following single and double interactions.
- Fig. 11 Photo of remaining tin disc following a single interaction.
- Fig.12 Schematic of narrow channel confinement in cylindrical tank.
- Fig. 13 Schematic of wedge shape confinement in cylindrical tank.
- Fig. 14 Schematic of double width channel.
- Fig. 15 Pressure recorded during propagating interaction in double width channel.
- Fig. 16 Single frames of Hycam film illustrating self-sustained propagation of interaction in stratified tin/water system.
- Fig. 17 Schematic of vapor explosion propagation.
- Fig. 18 Pressure recorded during propagating interaction in narrow channel.
- Fig. 19 Schematic of potential flow of water above explosion zone.
- Fig.20 Pressure variation in water from potential flow model of wedge.
- Fig.21 Pressure recorded illustrating failure of propagation in narrow channel for a water height of 5 cm.
- Fig.22 Schematic of one dimensional expansion of thin vapor layer under water column.
- Fig.23 Effect of water height on pressure decay of one dimensional vapor layer below water column.
- Fig.24 Schematic of propagating interaction subjected to a sudden change in confinement, creating curvature of the interaction front.
- Fig.25 Comparison of pressure decay ahead of planar and spherical interaction front.
- Fig.26 Schematic of cylindrical potential flow model.
- Fig.27 Comparison of pressure variation in water from potential flow models of wedge and expanding cylinder.

- Table 1 Characteristics of single interactions.
- Table 2 Effect of geometry on interaction energetics.

NOMENCLATURE

Α	Suface area of melt
Во	Bond number
C_d	Coefficient of drag

Force applied against water

F(z) Potential function g Acceleration of the drop

H_w Water height I Impulse

k Thermal conductivity of melt

KE Kinetic energy m Mass of water n π / sector angle

P Pressure

Ps Pressure at cylinder surface

 P_{∞} Ambient pressure

Q Heat flux
r Radial distance
R Cylinder radius
T Temperature

T_i Interfacial temperature

t Time

teq Time for coolant and drop velocities to equilibrate Water flow velocity

U Water flow velocity
U Internal energy

U_∞ Uniform flow velocity of water

V Velocity of water

W Work

We Weber numbrr

x Distance along x coordinate y Distance along y coordinate

α Thermal diffusivity
 φ Velocity potential
 γ Perfect gas constant

θ Angular position in wedge flow model

ρ Density of water
 ρ_c Density of coolant
 ρ_h Density of hot liquid
 σ Surface tension

Subscripts

c Cold liquid h Hot liquid

1.0 INTRODUCTION

In the event that a cold liquid and a relatively much hotter one come into contact there is the possibility of a violent explosion. This type of explosion results from the sudden vaporization of the cold liquid as it is heated by the hot one. The phenomenon is referred to as a vapor, steam, physical or thermal explosion. In particular, it is known as a rapid phase transition when the explosion involves a cryogenic liquid, and a fuel/coolant interaction when associated with a core meltdown in a nuclear reactor.

There are a number of industrial scenarios where accidental vapor explosions have been reported, as described in the summaries of Buxton and Nelson (1975) and Reid (1985). These have occurred in foundries, primary aluminum and steel plants, paper mills, under circumstances involving the mixing of water with molten steel, aluminum or salt mixtures (smelt). Vapor explosions have also been observed in pouring liquefied natural gas (LNG) into water and therefore are a risk in the marine transport and harbor unloading of LNG. Of great concern today is the safety risk of nuclear reactors in the event of a loss of coolant accident. The overheating of the reactor core leads to the melting of the fuel, risking a thermal interaction between the hot molten fuel and the coolant. The violent vaporization of the coolant could produce over pressures of sufficient strength to rupture the reactor vessel, allowing the release of radioactive products. Finally, one of the most disastrous examples of a vapor explosion took place naturally in the last century, when huge amounts of water and lava mixed during the Krakatoa volcanic eruption. The result is noted as the largest terrestrial release of energy in recorded history.

Typically, in such accident scenarios, the hot and cold liquids come into contact to form either a coarse mixture of fuel fragments blanketed in a vapor film and dispersed in the coolant, or a stratified mixture with a vapor film separating the two layers of liquids. The collapse of the vapor film (in both cases) brings the two liquids into direct contact. Very rapid heat transfer follows accompanied by fine fragmentation of the fuel, which produces particles in the range of $50-100 \mu m$. This fragmentation is an essential step because it provides the increase in surface area required for the characteristic high heat transfer rate. As a result, rapid vaporization occurs, with little change in volume, yielding high pressures in

the form of impulsive shock loading. The event is commonly summarized by the following four distinct phases through which a vapor explosion progresses (Corradini et al., 1988):

- 1. Premixing The two liquids are initially at temperatures such that a thin vapor film forms effectively shielding the cold liquid from the hot one.
- 2. Triggering The local collapse of this vapor layer, either due to an external disturbance or to a growing instability in the system (boiling dynamics), causes direct liquid-liquid contact entailing high heat transfer rates and local sharp pressure rises.
- 3. Propagation This high pressure pulse can travel through the entire mixture resulting in a coherent energy release. The pressure pulse promotes the collapse of the adjacent vapor film and fine fragmentation and mixing of the two liquids.
- 4. Expansion The sudden vaporization of the cold liquid produces high pressure vapor which can cause mechanical damage to the surroundings as it expands.

The aim of the experimental and theoretical work carried out by vapor explosion researchers is to acquire a better understanding of the physical processes occurring within each of these four steps, in order to determine the necessary criteria for the onset and support of a vapor explosion, and the energetics associated with the event. To this end, different liquid/liquid systems have been studied in a variety of configurations (single drop, coarse mixture of melt fragments in coolant, stratified melt/coolant layers). The basic mechanisms involved in the interaction have been identified and understood independently of one another. However, still lacking is an understanding and description of the combined effects produced by the various mechanisms. Although many vapor explosion models have been put forward, none have been completely successful in accounting for all experimental results, especially concerning large scale events.

In the sections to follow, theoretical aspects and the relevant experimental work pertaining to the various stages of a vapor explosion are presented, ending with the aim of this particular study. Comprehensive reviews of vapor explosion studies can be found in the works of Cronenberg and Benz (1980) and Corradini et al.(1988).

1.1 Spontaneous nucleation theory

The spontaneous nucleation theory was proposed by Fauske (1973) as a criterion for the existence of a vapor explosion. The model considers that an explosive interaction is possible provided the interface temperature at the moment of contact exceeds the spontaneous nucleation temperature, T_{sp} . Based on conduction theory, the contact temperature at the interface, T_i , is determined by the following expression:

$$T_{i} = \frac{T_{h}(k/\alpha^{1/2})_{h} + T_{c}(k/\alpha^{1/2})_{c}}{(k/\alpha^{1/2})_{h} + (k/\alpha^{1/2})}$$
(1.1)

where T is temperature, k and α are the thermal conductivity and diffusivity respectively, and h and c subscripts denote the hot and cold liquids.

As shown in fig.1, the nucleation rate remains low until the temperature of the liquid reaches a critical value. At this point minimum size, stable vapor embryos are produced, associated with a sudden increase in the nucleation rate. When the vapor nucleation occurs in the bulk of the liquid, due to molecular density fluctuations, this temperature limit is called the homogeneous nucleation temperature. It corresponds to the limit of superheat and is approximated to be about 90% of the critical temperature. When nucleation sites are available the limit of spontaneous nucleation is lower, resulting in heterogeneous nucleation of the liquid. In Fauske's theory, the vapor generation rate associated with this regime for a volume of liquid is presumed to be sufficiently fast to produce shock waves.

The strongest support of Fauske's spontaneous nucleation theory is found in experiments involving cryogenic liquids (Nakanishi and Reid, 1971; Enger and Hartman,

1972). The spontaneous nucleation requirement was consistently valid with various mixtures and spill sizes. However, some experimental evidence is at a variance with this criterion. One example is the mixture of uranium dioxide (UO₂) and sodium (Na) used in liquid metal cooled fast-breed reactors. The contact interface temperature is well below the spontaneous nucleation temperature of Na and therefore precludes the possibility of a vapor explosion. However, experiments carried out by Anderson and Armstrong (1972) have demonstrated that this pair does produce vapor explosions. The results indicate that a vapor explosion does not occur immediately upon contact but after a finite delay. The delay, as suggested by Fauske (1973), is due to the superheating of Na globules in the UO₂, until they reach the spontaneous nucleation temperature. The subsequent rapid vaporization results in the explosions observed. In addition, the experiments of Nelson and Buxton (1978) using uranium dioxide and iron (2000K) in water (300K), which gave an interface temperature T₁ (1650K) greater than the critical temperature of water, produced vapor explosions. This result cannot be justified on the basis of vapor bubble nucleation as the controlling mechanism.

Although the spontaneous nucleation theory is subject to criticisms it nevertheless helped focus attention in the understanding of thermal explosions. It is recognized that its role may be very localized (i.e. involving the superheating of a very thin layer of coolant), yet to be clearly demonstrated experimentally. A further hindrance in assessing this theory is the difficulty in determining the actual $T_{\rm Sn}$ of a liquid, which is sensitive to the surface conditions, the presence of impurities, etc.

1.2 Vapor film stability and triggering

1.2.1 Vapor film formation

The nucleation step associated with the heating of a liquid occurs because vapor embryo bubbles of a minimum size are produced. Below a critical size they are unstable and tend to collapse. If a sufficiently large number of vapor embryos are generated over a surface area (10⁹/cm²), they can coalesce due to physical interference and form a vapor blanket separating the two liquids (Reid, 1983). The interface temperature required for such

a film to form is the minimum film boiling temperature, in the case of a heated pool of liquid, or the Leidenfrost temperature, applied to discrete liquid drops. This temperature is identified on the heat flux curve in fig.2, corresponding to the point of minimum heat flux or very long vaporization time. An example of this behavior has been observed in LNG/water experiments (Reid,1983). These two liquids interact explosively as predicted by the spontaneous nucleation theory, however, when the water temperature is significantly higher than T_{Sn}, they rarely produce an explosion. In this case the high water temperature leads to the rapid establishment of film boiling, creating a thin vapor layer of low thermal conductivity which effectively shields the bulk LNG from the water.

The film boiling regime represents a relatively quiet and inefficient mode of heat transfer. It is characterized by a regular "pinching off" of vapor bubbles in time and space which condense on the colder surface, while the hotter one feeds more heat to maintain the vapor layer. The thickness, which lies in the range of 10^{-8} - 10^{-5} m, is not typically uniform over the entire surface area due to instabilities associated with the boiling dynamics at the top surface (vapor bubble departures, vapor/coolant interface ripples) and any temperature gradients in the coolant or melt (e.g. variations in the melt thickness; edge heat losses) (Naylor, 1985).

1.2.2 Vapor film destabilization

Provided the interface temperature between the melt and the coolant is above the minimum film boiling or Leidenfrost temperature, a vapor blanket will form preventing direct liquid-liquid contact. The collapse of the vapor film is referred to as the triggering event of a vapor explosion, initiating the direct contact of the liquids. The stability of the vapor film depends on the system conditions, such that the local or complete collapse may occur "spontaneously", due to the system's own fluctuations, or be triggered externally by a disturbance generated to the system.

Spontaneous trigger

To the eye the vapor film appears continuous, however, studies by Yao and Henry (1978) have confirmed that brief random contacts appear throughout the film boiling regime. These become longer lasting and more numerous as the minimum film boiling temperature is approached, corresponding to a minimum vapor film thickness for which a stable film cannot

be sustained naturally. The process of spontaneously triggered film collapse is described by the following three stages: 1) thinning of the vapor film; 2) penetration of tongues of liquid; 3) spreading of the contact region (Bankoff, 1980).

Experimental observations of spontaneous film collapse between liquid pairs have been conducted by Dullforce et al. (1976). They investigated the spontaneous film collapse of molten tin drops released in water at various coolant and melt temperatures. The results of their study are summarized in fig.3, which identifies the conditions when spontaneously triggered interactions occurred. The interaction zone is defined by three boundaries: the bottom horizontal boundary marks the freezing temperature of water; the vertical boundary corresponds to a melt temperature of 573K, relatively close to its freezing temperature (505K); and the diagonal boundary qualitatively separates conditions of thick and thin vapor films. They also measured dwell times before film collapse and noticed the time increased rapidly as the upper diagonal boundary of the interaction region was approached. It is proposed that this delay represents the necessary time for the melt surface temperature to reach the limiting value for which the film becomes unstable. Corradini (1978) offers an interpretation of the upper diagonal boundary based on the time required for film collapse and that required to reach the saturation temperature of the water, at the film interface. During the film collapse time, heat is transferred from the melt to the water such that it attains its saturation temperature. If the time for film collapse is shorter than the evaporation time then sufficient liquid-liquid contact is achieved resulting in an explosive interaction. However, if the time for film collapse is longer than the saturation time, the water will evaporate fast enough to reinforce the vapor film layer, preventing extended liquid-liquid contact.

External triggering

The collapse of the vapor blanket can also be prompted by an external trigger which generates a mechanical disturbance to the system. The disturbance, in the form of a shock wave, collapses the film locally and forces the two liquids into contact. The shock wave is characterized by its magnitude and duration (impulse) and must be sufficiently strong to completely collapse the film over the time period required for the vaporization of the cold liquid. In this manner a vapor explosion can be initiated.

There are several ways to trigger thermal explosions externally. Board and Hall (1974) conducted experiments with tin contained in a shallow crucible under water.

Interactions were triggered by a pressure pulse of ~1 MPa generated by rupturing a diaphragm connecting the pressurized apparatus to the atmosphere. In another experiment where tin was poured in a narrow trough, interactions were initiated by applying an impulse at one end of the trough by striking it with a hammer. The vibration of the rod generated shock waves which collapsed the vapor film.

Frolich and Anderle (1980) investigated the initiation of a vapor explosion by high voltage discharge through an exploding wire. A spherical shock wave was generated (ranging between 2.0 and 6.0 MPa) causing the two liquids to come into direct contact. According to their high speed spark photography results, the shock wave did not fragment the molten drop in film boiling, but merely produced a sufficient instability to disrupt the vapor layer.

The requirements of the trigger naturally depend on the stability of the initial configuration. A more detailed look at the triggered film collapse was carried out by Naylor (1985) in his experimental studies of film destabilization over a heated brass rod. His findings reveal the existence of a thermal threshold above which permanent film destabilization is not achieved. As the rod temperature increases, the coolant temperature for which complete collapse is possible decreases. Above the threshold only transient film collapse was observed as the film boiling regime was quickly re-established.

Nelson and Duda (1982) also made trigger requirement inquiries for the case of molten iron-oxide drops (~ 2000K) subjected to over pressures in water. The effect of the over pressures was investigated by varying the distance between an exploding wire and the drop. They reported a threshold pressure of .4 MPa below which explosions could not be triggered. At the threshold pressures of .2 and .4 MPa, they observed delays of up to 100 ms before actual film collapse.

To date, the detailed role of film destabilization in a vapor explosion is not adequately understood. The presence of the vapor film delays the interaction, however, the oscillations of the film or sudden collapse can induce fragmentation of the melt. Bjornard et al. (1974) recorded the oscillatory pressure signals generated from tin/water interactions, and found that the duration frequency and magnitude of the pressure pulses were influenced by the initial tin and water temperatures. This suggested to them that the fragmentation mechanism is linked to the dynamics of the vapor film surrounding the drop. It is therefore perhaps one of the key steps in the initiation of a vapor explosion.

1.3 Fragmentation and mixing

Based on the characteristics of observed vapor explosions, the thermal energy transfer must proceed over a very short time period. The duration is in the order of ms corresponding to the time between film collapse and the high pressure generation. Such high rates of heat transfer imply that fragmentation and rapid mixing of the two liquids is an essential step.

According to the classical diffusive beat transfer calculations of Witte et al. (1970), it is shown that heat transfer rates 10^3 times that of normal boiling processes are required to account for the vapor production rates of a thermal explosion. Evidence of the required fragmentation is manifested by the fine particle debris collected following an explosion. In the event that a vapor explosion is not successfully triggered, the melt (if solid at ambient conditions) solidifies into one piece, i.e. no surface area enhancement. On the other hand the product of an energetic interaction is the finely fragmented debris. Debris analyses, performed in the experiments of Nelson and Duda (1982) using an optical image analyzer, revealed that fragments as small as 1-250 μ m were produced. Their calculations, based on projected surface areas, assuming particles of circular area, estimate that 2.9 mm iron-oxide droplets break up into millions of fragments

Of pertinent interest to vapor explosion studies is how the hot liquid breaks up in a time as short as that of the explosion. Since this is a fundamental aspect of the heat transfer stage it has stimulated much speculation. What are the physical processes occurring during the observed delay time between triggering and the explosive interaction, which provide the conditions for the rapid vaporization? Many theories have attempted to answer this question. In general they are classified under two broad categories depending on the driving force for fragmentation: those related to hydrodynamic effects and those related to thermal effects. The following describes the physical processes involved while a few of the most accepted fragmentation theories are described in App. A. Comprehensive reviews on fragmentation can be found in Cronenberg and Benz (1980) and in Corradini et al. (1988).

1.3.1 Hydrodynamic effects

Hydrodynamic fragmentation takes effect when a molten droplet is subjected to velocity induced surface forces, sufficient to disrupt the cohesive action of surface tension. The potential to cause the break-up of the drop in this situation is expressed by the Weber number, We, which represents the ratio of inertial to surface tension forces. It is expressed as:

$$We = \frac{\rho_c U_{rel}^2 D}{\sigma}$$
 (1.2)

where ρ_c is the density of the cold liquid, U_{rel} is the relative velocity between the two liquids, D is the drop diameter and σ is the interfacial surface tension.

If the Weber number exceeds a critical value then the inertial forces overcome the surface tension and the drop breaks up into smaller more stable drops. The break-up forces are either due to one or a combination of possible fragmentation mechanisms. If two fluids having a common surface boundary are accelerated in a direction from the lighter fluid towards the heavier one, perpendicular to the boundary, interface irregularities will tend to grow. This effect is known as Rayleigh-Taylor instability. The Kelvin-Helmholtz instability arises at the interface between two fluids when a parallel relative velocity exists between them, inducing the layers to mix through the formation of eddies. And finally, material may be stripped off the drop due to the shearing effect of the tangential component of flow over the surface, which is termed boundary layer stripping.

Flow induced drop break-up experiments have demonstrated these hydrodynamic effects for liquid drops in both gas and liquid mediums. However experimental evidence has shown that significant fragmentation occurs in situations where the velocity differentials are relatively small, as in single drop experiments. Therefore, it is not expected that hydrodynamic effects alone are responsible for the fragmentation observed, although can enhance the process.

1.3.2 Thermal effects

Fragmentation mechanisms involving heat transfer are grouped under thermal effects. The processes involved are boiling dynamics which can produce sufficiently large forces to disrupt the melt surface; internal pressurization of the coolant as it penetrates, or is encapsulated by, the melt; and solidification of the melt inducing thermal stresses on its shell, creating fissures through which melt is ejected. Experimental work by Dullforce et al. (1976), using tin and water, has shown that the degree of fragmentation is affected in particular by the initial metal temperature. They noticed that the extent of the fragmentation increased with the metal temperature. Complementing such observations are the pressure data of Bjornard (1974). He recorded the pressures generated during tin/water vapor explosions and also reported an increase in intensity with higher melt temperatures. In both studies, the violence of the interaction increased up to a maximum melt temperature beyond which it dropped dramatically (i.e. ineffective vapor film collapse thereafter).

1.4 Propagation of vapor explosions

The majority of vapor explosion investigations, experimental and theoretical, pertains to small scale (single drop) events, focusing on the understanding of the detailed physical processes governing the interaction. However, especially in light of industrial safety considerations, the study of vapor explosions requires larger scale experiments to investigate the characteristics of the interaction: its propagation behavior and the energetics of such an event. Real-life incidents and experimental observations have demonstrated that large scale vapor explosions can be very violent, causing severe damage to the surroundings. This implies that either the interaction is triggered everywhere at once, or spreads from a localized area of initiation. The latter case has proven to be true since most triggers produce only a local disturbance, responsible for the initiation of the interaction. There are typically two melt/coolant configurations through which an interaction can propagate: a homogeneous mixture of vapor blanketed melt fragments dispersed in the coolant, and a stratified mixture where the melt and coolant are initially separated by the vapor film. The features of a propagating explosion front can be appreciated through the following experimental work.

1.4.1 Experimental observations of propagation

Coarse mixtures

Briggs (1976) at Winfrith studied aluminum/water and tin/water interactions using 20 kg of molten metal. A coarse mixture of fuel fragments in coolant formed in the lower half of the tank through which an interaction propagated rapidly, usually starting at the base of the tank. Propagation velocities in the order of 200 m/s were recorded, characterized by over pressures reaching 40 MPa. Briggs reported difficulties in establishing the "right" initial conditions for a violent explosion as many tests (~20) were unsuccessful.

Large scale coarse mixture explosions were performed at Sandia National Laboratories by Buxton and Benedick (1979), using thematically generated molten core melt simulant (iron alumina) and water in an open vessel. Most tests resulted in a spontaneous explosion, producing over pressures between 2 - 7 MPa with conversion ratios averaging 0.2 - 1.5 %.

Board et al. (1976) also conducted coarse mixture experiments by dispersing 2 kg of tin along a 1m long shock tube. A fast propagation front traveled up the tube at velocities of 100-250 m/s, generating over pressures of about 5 MPa (100 ms rise time; 100 ms pulse width). Based on the characteristics of the front and considering the velocities to be in the order of the sound velocity in a two phase mixture, they identified the propagating front as a shock wave.

Stratified mixtures

Board and Hall (1974) also conducted tin/water experiments in both a thin unconfined trough, immersed in water, and in a narrow channel (2.54 cm wide). In both cases the tin was allowed to settle at the bottom forming a stratified water/tin configuration. The interaction was triggered at one end. The explosion behavior observed in the trough consisted of local interactions which slowly traveled along its length. In the case of the more confined channel, a continuous propagation was observed moving at ~ 50 m/s along the length of the channel. They noted that the self-driven vapor blanket collapse allows the propagating fragmentation or mixing to occur, thus a sustained interaction. They also suggested that the more continuous propagation in the narrow channel is possible due to the increased dynamic constraint of the vessel.

Anderson et al. (1988) investigated the nature of stratified explosions in both horizontal and vertical geometries, using tin/water and freon/water mixtures. They discovered that the metastability of the horizontal configuration fluctuated uncontrollably, resulting in inconsistent responses to the trigger. To gain control over the stability conditions at the liquid/liquid interface, they placed a moveable diaphragm between two vertical liquid columns, freon and water, and initiated the interaction at the bottom. Explosions propagated upward at 90-150 m/s generating peak over pressures between 0.2 and 1.0 MPa. In an attempt to estimate how much material was involved in the interaction they calculated the total mixing depth. Assuming that two liquid layers of the same thickness mix and come to 100% equilibrium, a total mixing depth of 6 mm was required to generate the measured over pressures.

An investigation of scaling effects was carried out by Bang and Corradini (1988, 1990) in their stratified liquid nitrogen (LN₂)/water and freon/water experiments. The vessel dimensions used were in width, length and height respectively: $2.5 \times 20 \times 65$ cm and $6.4 \times 50 \times 150$ cm. The freon/water interactions were in general more violent than the LN₂/water, and escalated in the larger vessel to velocities between 70-100 m/s, producing overpressures varying from 0.2 to 0.8 MPa. It appeared that a vessel longer than 150 cm would be necessary for a steady propagating front to develop. From their films they estimated the depth of intermixing of the liquids to be < 1 cm. The depth of the overlying liquid was reported to affect the propagation behavior by influencing the extent of intermixing.

Stratified tin/water interactions have been studied by Ciccarelli et al. (1991) at McGill University. Propagating interactions were externally triggered at the end of a 1.27 cm wide channel, characterized by velocities of about 40 m/s and pressures varying between 0.2 to 0.9 MPa. They determined that a self-sustained propagation occurred when sufficient inertial confinement was provided by the mass of the overlying water. Self-sustained propagations were always observed at water heights above 12 cm, whereas at lower water heights (< 5 cm) propagations never occurred.

Most recently Sainson et al. (1993) of Gaz de France investigated the behavior of a vapor explosion in an initially stratified LN₂/water geometry. A relatively large experimental rig was used, 2.5 x.3 x.6 m in length, width and depth respectively. They discovered that the tendancy for an explosive interaction to propagate depended on the interface conditions: a wavy interface provided sufficient intermixing to sustain a propagation (~235 m/s), whereas

a propagation never occured in a well stratified system where an explosive interaction was limited to the trigger zone.

It is apparent from the experimental observations that an energetic, self-sustained vapor explosion propagation can occur in coarse mixtures, and also in stratified mixtures where it was formerly believed not possible due to the lack of premixing between the liquids. A number of questions arise of fundamental interest: what are the initial condition requirements for a propagation to develop; what are the controlling mechanisms which sustain the propagating front and what governs the amount of material involved in the interaction? The propagation in the coarse mixture is achieved as the pressure pulse generated by an exploding drop reaches an adjacent drop, causing its vapor film to collapse, fragmentation and subsequent vaporization of the coolant. In the stratified geometry the vapor film insulating the coolant from the melt is continuous, but similarly the pressure field generated from a local interaction must be sufficient to sustain a continual collapse of the vapor film. The propagation of the interaction is limited by the time for film collapse, mixing, transfer of thermal energy to the coolant and the subsequent vapor production. Because of the premixed condition in the case of the coarse mixture, the interaction is typically more energetic due to the larger surface area initially available, resulting in higher heat transfer rates. It seems that, based on many studies (e.g. Board and Hall (1974), Bang and Corradini (1990), Ciccarelli et al. (1991) a qualitative criterion for the pressure wave to be self-sustained is that the inertial confinement of the system be large enough to provide the necessary coupling between exploded and adjacent unexploded areas. This requirement is illustrated in Ciccarelli et al. (1991) where they measured pressure impulse decreases as the height of the water in the channel was lowered, as shown in fig.4. At some minimum water level, the pressure impulse is to weak (i.e. the pressure is relieved too rapidly) to sustain the continual vapor film collapse and the propagation fails.

1.4.2 Theoretical modeling of vapor explosion propagation

Two approaches have been adopted in the modeling of vapor explosions. One method is to consider the equilibrium thermodynamics and calculate the maximum expansion work which can be done by the vaporized coolant. Hicks and Menzies (1965) evaluated this to be about 30% of the thermodynamic yield. This prediction is in fact significantly higher than the conversion ratios calculated in real events which fall in the order of a few percent. In an effort to integrate the necessary conditions for the occurrence of a vapor explosion and

the physical phenomena and rate processes involved, a more mechanistic approach to the modeling has been pursued, incorporating the presumed characteristics of the heat transfer and fluid dynamics. The common feature of these models is that the pressure and flow fields, resulting from the energy release zone, cause a spatial propagation of the interaction through the mixture. Thus strong hydrodynamic coupling between the interaction zone and adjacent unexploded region is required. The main difference between these models lies in the fragmentation mechanism; how the surface area is enhanced as the pressure wave travels through the mixture.

Among the models reviewed are Fauske's (1974) nucleation model which is single in requiring the spontaneous nucleation criterion, Colgate and Sigurgeirsson's (1973) self-mixing model and Board and Hall's (1975) detonation model, upon which most subsequent modeling efforts are based. Finally Harlow and Ruppel's (1981) work is presented, consisting of a preliminary demonstration that a self-sustained propagation at a liquid/liquid interface is theoretically plausible.

Fauske's (1974) "Capture model"

The fundamental idea behind Fauske's (1974) model is the spontaneous nucleation criterion, therefore requiring an interfacial temperature above T_{SP}, as described in section 1.1. The concept is extended to account for large scale explosions as observed in the case of freon/oil mixtures. The model is composed of a capturing process and pre-explosion fragmentation stage. Essentially small droplets of coolant are "captured" and heated until they explode. The pressure wave generated, a shock wave, fragments larger drops to form a population of individual small droplets. When the number is large enough, the explosion of one droplet produces a pressure increase sufficiently elevated to "capture" and trigger the explosion of many droplets. The propagation mechanism is based on slow and incoherent shock wave fragmentation. Fauske enumerated three requirements for a vapor explosion:

- 1) breakdown of the vapor layer permitting direct liquid-liquid contact
- 2) immediate explosive boiling implying T_i must be $> T_{SP}$
- proper inertial constraint for the process to escalate on an a time scale required for a large mass explosion

Colgate and Sigurgeirsson's (1973) dynamic mixing model

Colgate and Sigurgeirsson (1973) proposed a theory on the mixing of molten lava and water, inspired by observations of seabed explosion craters. They suggested that a potentially explosive interaction occurs by a process of self-sustained mixing of the two liquids, resulting from the growth of instabilities. The event begins with an initial pressure release at the lava-water interface, large enough to "crater" the crust and drive a pressure wave radially along the interface. Because the pressure wave will travel faster in water than in the lava, an annular high pressure region will push down on the lava and back towards the rarefaction at the original point of cratering. This downward and inward acceleration of the lava water interface gives rise to both Rayleigh-Taylor instabilities, on account of the lighter water being accelerated towards the heavier lava, and Kevin-Helmholtz instabilities resulting from the velocity shear. These instabilities promote the interpenetrating or mixing of the two liquids. Simple order of magnitude calculations showed that these mechanisms could lead to fragmentation.

Board and Hall's (1975) thermal detonation model

The analogy between a chemical detonation applied to a vapor explosion was first suggested by Board and Hall (1975), based on their stratified tin/water experiments (1974). The classical picture of a chemical detonation consists of a shock wave passing through a homogeneous mixture of reactants. The reactants are compressed adiabatically, leading to a sharp rise in temperature which provokes an extremely rapid chemical reaction in a narrow zone behind the shock wave. The energy release from the chemical reaction sustains the shock wave as it propagates through the mixture of reactants.

In an analogous manner Board and Hall (1975) proposed that the shock wave in a thermal detonation causes the fragmentation and mixing of both liquids. The high pressure generated from the rapid heat transfer sustains a steadily propagating shock wave through the mixture. Therefore the analogy to the temperature increase in a chemical detonation, initiating the chemical energy release, is the film collapse and rapid surface area increase (resulting from the velocity differentials induced by the shock wave) preceding the heat transfer.

A criterion for the existence of thermal detonations is that they must satisfy the onedimensional conservation laws of mass, momentum and energy. Based on these laws and the equations of state, it is then possible to determine the downstream equilibrium states without any knowledge of the mechanical and thermal processes occurring in the reaction zone. Such calculations are referred to as Hugoniot analysis, which depend on the energetics of the interaction rather than the kinetics of the processes involved. This analysis applied to vapor explosion waves assumes that the wave is steady and that equilibrium conditions exist at the interaction zone boundaries.

The Hugoniot calculation specifies all possible equilibrium end states corresponding to various propagation speeds of the wave itself. In the case of chemical detonations an added criterion is imposed to obtain a unique solution of the wave speed, called the Chapman-Jouguet (CJ) condition. This condition demands that the downstream equilibrium flow is sonic relative to the wave, corresponding also to the minimum wave velocity and entropy change. The choice of this solution is justified from stability arguments (although the existence of such a wave cannot be proven based on physical principles). The same procedure is used to determine the wave speed solution of a thermal detonation although, without any knowledge of the wave structure, the stability arguments used to justify the solution choice may or may not be applicable.

Board and Hall (1975) performed Hugoniot calculations to make quantitative predictions of the behavior of tin/water interactions. They considered a one-dimensional normal shock wave traveling through a homogeneous mixture in which all of the hot liquid interacts with all of the cold liquid. They obtained steady-state solutions of wave speeds (~300 m/s) and over pressures (~100 MPa), which were generally higher than those ever observed experimentally. In order for such waves to be sustained the fragmentation induced must occur over a sufficiently short time scale such that the energy released goes into supporting the front. Board and Hall's fragmentation calculations are presented in Appendix B, shown to satisfy this requirement.

The detonation model has evolved since the first steady-state calculations performed. Subsequent researchers have developed models which do not require that all of the melt be fragmented at the end of the reaction zone, but rather introduce a new variable representing the fraction of melt that participates in the interaction. Also, transient models have been developed in an attempt to address more of the complexities of the physical processes occurring during a real vapor explosion. To date however, the propagation phase has been

modeled in an idealized homogeneous geometry and little theoretical work has focused on the propagation in less ideal geometries (e.g. stratified media).

Harlow and Ruppel's (1981) propagation calculations

The objective of Harlow and Ruppel's calculations was to verify whether a self-sustained propagating front could exist along a liquid/liquid interface. They incorporated the propagation mechanisms of Board and Hall's (1975) detonation model and Ochiai and Bankoff's (1976) splash theory (see App.A) into their conceptual picture of the propagation as shown in fig.5. The wave configuration travels to the right at a constant speed, with shock waves S1 and S2 traveling at a much greater velocity through the liquids than in the vapor region. They implode the vapor film, causing the interface to be deflected inwards and producing the transmitted shocks S1' and S2'. The interface is stable until these transmitted shocks reach the opposite surface at point A. At this point Rayleigh-Taylor instabilities arise in the region denoted by A-B, causing the two liquids to mix. With the increased surface area, heat is transferred in the zone B-C. At point C, vaporization of the coolant occurs driving the two liquids apart and supplying the necessary energy to support shocks S1 and S2. Based on symmetrical shocks, they performed numerical simulations of the event, showing that film implosion could sustain the mixing, heat transfer and explosive boiling typically characteristic of a propagating interaction.

1.5 Objectives and outline of present study

With the evidence provided by a number of experimental studies it is recognized that a self-sustained energetic explosion front can travel through an initially stratified fuel/coolant mixture. In order for the propagation to be continual and self-sustained, a coupling mechanism must exist which communicates the disturbance generated locally to the adjacent stable area of the mixture. The disturbance is transmitted through the pressure field (and associated hydrodynamic flow) in the liquids although the precise mechanistic details remain elusive.

The experimental observations of Ciccarelli et al. (1991), Board and Hall (1974) and Bang and Corradini (1990) have shown that a one-dimensional propagating front is self-sustained provided the interaction is sufficiently confined. This was demonstrated in the narrow channel containing a critical depth of water overlying the molten tin, creating a strong coupling.

Still lacking, however, is an understanding of the physical mechanisms governing the propagation of the explosion front in a stratified mixture. As an initial investigation towards this goal, it is of interest to study the behavior of the interaction in the absence of boundary effects and discover whether an initially unconfined interaction can propagate. This can be accomplished by initiating an interaction in the center of a large tank, the walls being remote from the early stages of the propagation. The aim of this study in particular is to verify whether a self-sustained propagation does develop in a stratified geometry in the absence of confining walls, and to characterize its behavior. To explore this question an experimental investigation using tin and water has been carried out and is presented in the next sections as follows:

Section II describes the experimental apparatus and procedure employed to study the details of the interaction.

Section III is a presentation of the experimental results.

Section IV contains a discussion of the results and observations.

The conclusions drawn from this study are finally presented in section V.

2.0 EXPERIMENTAL FACILITY AND INSTRUMENTATION

The first step in the experiment is to form a stable stratified mixture of tin and water. When they are at their appropriate temperatures, the tin is released from the heated crucible into a water filled cylindrical tank. The interaction is triggered at the center of the tank and the event is recorded using high speed cinematography, and fast response pressure transducers.

A schematic diagram of the entire experimental set-up is shown in fig.6. Approximately 4 kg of tin are melted in a graphite crucible and heated to about 800°C within two 1250 W semi-cylindrical peramic ovens, placed face to face to form a closed cylinder. The temperature is monitored by a chromel-alumel thermocouple dipped into the molten tin. When the appropriate tin and water temperatures are attained, a conical graphite plug located at the bottom of the crucible is manually lifted. The tin flows through a 2.54 cm diameter Teflon tube directed into the water filled cylindrical tank, forming a ~1 cm thick layer of tin at the base. Due to the large amounts of molten tin used, the cylindrical tank is enclosed in a 1 m steel spherical pressure vessel in order to prevent the violent dispersal of tin and water during the interaction. The vessel has vent holes in order to release the high pressure steam and windows (30.5 cm in diameter) for the visualization. One window is located on the top of the vessel and two others are positioned one on each side of the vessel. The cylindrical tank, shown in fig.7, is constructed of a 33.0 cm diameter base with a recessed 29.2 cm diameter in which a Teflon base is fastened. The Teflon base is high temperature resistant, reducing the heat losses of the tin. The actual area over which the tin layer spreads is 27.30 cm in diameter. The wall of the container is made of .317 cm Lexan sheet bonded at its edges. In light of the destructive nature of the explosions, this construction proved the simplest as the Lexan could be sealed back together after each explosive interaction. The height of the tank is 23.0 cm. Prior to discharging the tin, the tank is filled with boiling water which is allowed to cool to the required temperature in the low 70's °C.

The vapor explosion is externally triggered at the center by a shock wave which causes the initial film collapse. The spherical shock wave is generated by discharging a high voltage capacitor, $.2 - .4 \,\mu\text{F}$ charged up to ~20 kV, triggered by a switching spark gap. The energy is discharged through a thin copper wire attached to two electrodes, which are

immersed in the water 3.3 cm above the tin layer. Peak over pressures in the range of 2 MPa are produced ~ 3 cm away from the trigger. To reduce the decay in the shock strength, a cylindrical Delrin tube was mounted over the electrodes, thus focusing the shock ~1 cm above the tin surface. The trigger was activated after the molten tin had settled at the bottom of the cylindrical tank, forming a stable stratified layer.

The pressure-time history associated with the explosive interaction was recorded using fast-response piezo-electric pressure transducers. These transducers are PCB model 113A24 with either 5 or 10 mV/psi nominal sensitivity and a 1 µs response time. They are flush-mounted in water tight Delrin plugs which in turn are vertically mounted within brass cylinders extending into the water. As shown in fig.6, six transducers are located symmetrically across the diameter, spaced 3.8 cm apart and suspended 3.7 cm above the tin surface. The pressure information is recorded with a PC-based data acquisition system, including a multi-channel A/D board, at a frequency of 1 MHz and 1 µs resolution. The scope system is externally triggered by a Rugowski coil, activated by the high voltage discharge.

The explosive interaction was visualized with a Hycam 16 mm high-speed camera running at 2000 frames/second. Kodak high-speed 500 ASA 7296 color movie film was used. The camera was aligned in either of two positions: one provided an overhead view of the interaction through mirror deflection, the second viewed the interaction horizontally from the side. Lighting for the cinematography was furnished by two Lowel DP 1000 W flood lamps, located inside the pressure vessel, behind the cylindrical tank. Valuable information on the energetics of the interaction was also derived from the tin debris, collected after each trial and sieved to give the breakdown of fragment sizes.

3.0 EXPERIMENTAL RESULTS

The experimental results presented in this section are divided into four main parts. They address the determination of the initial conditions, the effect of the open geometry on the interaction characteristics, the triggering features of the interaction and the stability of the explosion front.

3.1 Initial conditions

The preliminary objective of the experiment was to obtain the initial conditions which allow the tin and water to form a stable, stratified configuration. As mentioned the vapor film stability is a function of the liquid temperatures and forms when the interfacial temperature is roughly the minimum film boiling temperature, which is about 300°C for water. Above this temperature the vapor film develops immediately upon contact with the water, preventing excessive heat losses of the tin during its descent to the base of the tank. Of consideration in attaining a stable condition is also the turbulent delivery of the tin into the tank. At too low a water temperature a spontaneous explosion would occur with the abrupt contact of the tin and the water (film destabilization). The appropriate water temperatures for tin at $\sim 800^{\circ}$ C were determined to be in the low 70's°C. These temperatures correspond to an interfacial temperature of $\sim 696^{\circ}$ C, well above the minimum film boiling temperature of water. At higher water temperatures, $T_{W} > 75^{\circ}$ C, the interaction was never triggered as the relatively thick vapor film could not be successfully destabilized.

3.2 Characteristics of the interaction

Information on the characteristics of the interaction were gathered for the 21 trials successfully performed, based on the high speed films, the pressure traces, and the tin debris. The most notable feature of the interaction was its highly erratic behavior: under the same experimental conditions three types of behavior were observed. In 9 of the trials an interaction was not triggered at all and a spontaneous explosion occurred later on or the tin froze. In the event of a spontaneous explosion it took place 10's of seconds later, randomly

initiated during the transitional or nucleate boiling regime. In the other cases where an interaction was successfully initiated, either a single, somewhat concentric, radially propagating interaction was observed (4 out of 12 interactions), or the explosion consisted of a first interaction followed by a second more energetic one (8 out of 12 interactions).

First interaction

Although the event sometimes consisted of two interactions, it is the first interaction which is of greater interest since it occurs in the stratified configuration, whereas the second one propagates through a coarse mixture of lofted tin fragments and water.

The interaction was filmed through the top window of the vessel, in order to distinguish the shape of the interaction front as it traveled from its central initiation point through the mixture. The resolution of the picture was relatively poor as the vapor bubbles produced during the film boiling regime blurred the view through the water. Also, the intensity of the interaction front was mild, further reducing the visibility. Under these circumstances a faint trace delineating the explosion front could be detected on some films and the ejection of the water, against the cross bar over the tank and against the side wall, was indicative of the front's motion. From this top view it was apparent that a somewhat concentric interaction front developed. This radially outward moving front had a certain degree of asymmetry, confirmed by the unevenly timed thrust of water against the side of the tank.

The profile of the growth of the interaction zone, visualized from the side of the tank, is reproduced from the high speed film in fig. 8. The interaction, initiated at the center of the shematic, appears as a cloud of vapor (the expansion zone marked by the black line) which grows spatially over time as the explosion front travels radially outward. The expansion zone is composed of a multi-phase mixture of molten and solidified tin fragments, water droplets and vapor. It is delineated by the interface separating the expanding high pressure vapor from the overlying water and the base of the tank. The rapid production of vapor, following the local interaction of tin and water, causes an upward thrust of water and generates a pressure field within it. This pressure impulse induces the collapse of the adjacent vapor film, resulting in the spatial motion of the explosion. While such a profile is clearly visible on the high speed films, the details of the dynamics within the vapor dome and of the vapor film collapse process are not discernable: the sudden production of vapor at the

leading edge of the interaction blurs this view. The first interaction, which takes place within the first 18 ms in fig.8, does not travel across the entire surface area of the tin, but stops about 10 cm from the center. The front is inclined at roughly 15° in its first stages of propagation, gradually becoming steeper (~ 30°) as it reaches this distance, where it then is idle.

The main characteristics of the first interaction: velocity of the propagation, overpressures and proportion of tin fragments smaller than 1 mm, are listed in Table 1. The pressure magnitudes recorded ranged between 0.15 and 0.5 MPa, represented by a typical pressure trace shown in fig.9. Transducers #1, 2 and 3 were located along a radius on one side of the cylinder while transducers #4, 5 and 6 were positioned along a diametrically opposite radius. Evidence of a propagating event is suggested by the temporal shift, on i oth sides of the cylinder, of the pressure pulses in the radial direction. Such values present an idea of the order of magnitude of the over pressures generated, since the pressure transducers suspended above the tin surface are inherently intrusive to the hydrodynamic flow of the interaction, thus distort the profile of the pulse. The asymmetry effect is also apparent in this trace as the interaction appears to travel earlier under pressure transducers #4, 5, 6, than under transducers #1, 2, 3. Based on these traces and the films, the average velocities of the propagation fell in the range of 30 to 60 m/s, with an average value of ~50 m/s. It should be noted that the asymmetry of the explosion front introduces a tangential component to the hydrodynamic flow. Therefore, the velocities measured from the pressure traces could overestimate the actual radial propagation speed.

In the event of an explosion a range of tin fragment sizes are produced, indicative of the violence of the interaction. In general, approximately 6% of the total tin mass was fragmented to particles < 1mm. The average fragment size breakdown for single interactions is given in fig.10. This distribution shows that only a thin layer of tin participates in the interaction while the remaining tin solidifies into a disc at the base of the tank. The appearance of the surface of the disc also confirmed that the interaction sometimes propagated in a preferential direction, with the extent of fragmentation varying over the tin disc area. A photograph of a post-explosion tin disc is presented in fig.11, displaying an example of the more extensive fragmentation in one particular area (right side of the disc).

Dynamics of a double interaction

As noted above, many of the explosions consisted of two interactions: the second one being much more energetic and destructive than the first. The horizontal view offered an interesting account of the dynamics of the entire explosion. From this view it was observed that the first interaction traveled radially outward to some maximum radius, at which point it was halted. After a delay of about 20 ms, as seen in fig.8, a second interaction propagated throughout the entire mixture, originating in the coarse mixture of tin fragments and water. During the time of the first interaction, the top surface of the water was accelerated upward and then downward again to a minimum point, corresponding to the start of the second explosion. For the occurrence of a second interaction, sufficiently hot molten tin fragments must be lofted in the wake of the first interaction, and some of the water must remain in the tank. There was no discernible pattern to predict the likelihood of the second interaction happening, except that it never occurred at water temperatures above 73°C. Evidence of the energetics is demonstrated by the tin debris size breakdown in fig.10, which in comparison to a single interaction, indicates the more extensive fragmentation resulting from a double interaction. Fragments smaller than 1 mm formed 19% of the total debris versus 6% for the single interaction.

3.3 Features of the initiation stage of the interaction

A typical characteristic of the pressure traces recorded is a delay between the triggering and the actual commencement of the spatial propagation of the interaction. High speed films taken from the side view revealed that the initiation of the explosion was accomplished by cyclical vapor bubble growths and collapses, following the generation of the triggering shock wave. Over a period of about 5-15 ms, vapor bubbles grow and collapse over the tin surface, escalating into an increasingly large disturbance in the vicinity of the trigger. This activity is noted during the first 5 ms in fig.8. However, the system displayed an erratic response, as only 12 out of the 21 trials resulted in energetic interactions. In many cases the initial disturbance generated by the trigger decayed without any significant effect. Thus, in an attempt to increase the effectiveness of the initial shock wave, it was thought that the initiation area should be more confined. This was accomplished by placing a thin Teflon disc (7 cm in diameter with a hole in the center) over the tube in which the

exploding wire was located, parallel to the tin surface. An initial successful triggering of the interaction only proved whimsical; this alteration did not work consistently.

An alternative idea to the method of triggering consisted of initiating an interaction in a confined area, which projected into the open, unconfined region. A narrow channel (1.9 cm wide x 7.6 cm long) was added at the edge of the cylindrical tank as shown in fig.12. The exploding wire was positioned at the edge of the tank inside the channel. Upon triggering an interaction was observed in the channel, however, it was not sustained as it reached the unconfined region of the tank; it failed immediately.

The small channel was replaced by a wedge, as depicted in fig. 13, in order to produce a stronger explosion front (larger disturbance) entering the unconfined region, while preserving the confined region for the initiation of the interaction. The wedge spanned half the diameter of the tank, 1.9 cm wide at its apex and 7.6 cm wide at the exit (23.6°). The trigger was positioned at the apex. Although a clearly visible interaction took place in the vicinity of the trigger, it did not develop into a propagation.

3.4 Perturbation of the interaction front

From the preceding results it is evident that the initiation of a propagating vapor explosion in an unconfined geometry is difficult to achieve. Failure of the interaction to develop into a sustained propagation in a diverging geometry, the inability to transit from a narrow channel to the unconfined region or to develop in the wedge geometry bring to question the effect of an expansion perturbation on the interaction front.

In order to investigate this aspect more carefully, an experiment was devised to study the behavior of a propagating interaction front when subjected to a sudden perturbation. The experimental apparatus used is shown in fig.14, consisting of two channels of different width, water-tight connected end to end. The idea is to investigate the behavior of the interaction as it travels from the narrow channel (1.25 cm) to the wider one (5.0 cm). The experimental procedure is much like that of the cylindrical tank experiment: the hot tin, heated to 750°C - 800°C, is poured into the water filled channels, at ~85°C, and allowed to settle to form a stratified configuration, the interaction is then triggered at the end of the 1.25 cm channel, by HV discharge through an exploding wire. A steadily propagating interaction

develops. Windows in the side walls of the channels allow the event to be visualized using high speed photography (Hycarn camera), and the over pressures generated are recorded by 5 piezo-electric pressure transducers, flush mounted along the side walls of both channels. Transducers #1, 2 and 3 are located in the narrow channel and transducers #4 and 5 are in the larger channel, spaced from left to right as shown in fig. 14.

A typical pressure trace of the three trials successfully performed is shown in fig.15. A propagating interaction is clearly recorded in the narrow channel, traveling at velocities ranging between 35 and 45 m/s which are characteristic of narrow channel stratified interaction propagations. However the sudden perturbation at the transition causes the propagation to fail in the wider channel, as testified by the absence of pressure rises for transducers # 4 and 5.

4.0 DISCUSSION

4.1 Highly confined propagation in a narrow channel

The motivation to explore the behavior of the stratified tin/water interaction in a cylindrical geometry stems from earlier investigations by Ciccarelli et al. (1991), which confirmed the importance of inertial confinement in the support of a propagating interaction within a narrow channel. The consistent behavior of the interactions in the stratified media revealed some of the characteristic features of a propagating interaction in a highly confined geometry. These experimental findings provide a groundwork for the understanding of stratified vapor explosion propagations and the influence of inertial confinement on the propagation. They are therefore first reviewed before extending to the unconfined condition in the cylindrical tank.

4.1.1 Characteristic features of the propagating interaction

The narrow channel interaction is triggered at one end of the channel and propagates along the entire length, with characteristic features exhibited by the high speed films and pressure records. From the Hycam reproductions of the propagating interaction shown in fig.16, the interaction appears as a wedge-shaped front (inclined at ~10°) which travels at a typical velocity of 40 m/s. A schematic of the interaction is illustrated in fig.17, formed by a high pressure leading edge and expansion zone in its wake. Following the local collapse of the vapor film, the water and tin come into contact and the subsequent heat transfer superheats a thin layer of water which undergoes a rapid phase change. The expansion of this high pressure vapor distorts the surface of the tin, and entrains molten and solidified tin fragments and water droplets downstream of the leading edge of the interaction. As the vapor expands and the water is thrusted upwards, a pressure and flow field is generated in the water ahead of the leading edge of the interaction. This disturbance causes the collapse of the adjacent film, resulting in the spatial propagation of the interaction. A typical pressure trace of the event is shown in fig.18. The pressure field in the water is described by the slow rise time of ~1 ms and peak pressures ranging between 0.2 - 0.9 MPa.

4.1.2 Energetics of the interaction

Based on the debris analysis following the explosive interaction only a small fraction of the initial tin volume participates energetically in the interaction. Assuming that fragments smaller than an arbitrary size of 1 mm contribute energetically to the interaction, the calculated tin layer thickness is < 2 mm. Further fragmentation of the tin results from the hydrodynamic shear flow in the wake of the interaction zone, where the molten tin fragments lose their heat slowly and do not participate energetically in the interaction. An estimate of the explosion yield can be made, which represents the amount of thermal energy converted to mechanical energy. The mechanical energy can be calculated directly from the velocity of the slug of water, or indirectly based on the mechanical impulse imparted to the water, as described by the pressure profiles. Assuming one dimensional flow and applying Newton's first law to the slug of water, the velocity, V, can be determined as follows:

$$V = \int \frac{Fdt}{m} = \frac{A \int Pdt}{m} = \frac{AI}{m}$$
(4.1)

where the impulse, I, is $\int Pdt$, A is the surface area over which the pressure pulse acts and m the mass of the slug of water. Substituting V into the expression for the kinetic energy then gives:

$$KE = \frac{mV^2}{2} = \frac{(AI)^2}{2m}$$
 (4.2)

The energy yield per unit surface area calculated from the vertical velocity of the water is 0.31 J/cm², and 0.26 J/cm² based on the recorded pressure traces. The conversion ratio, defined as the ratio of the kinetic energy of the tin and water to the sensible enthalpy of the tin, may also be evaluated. Assuming the tin is set into motion with the same velocity as the water, a conversion ratio of .063% is obtained based on the total thermal energy of the tin. If only the thermal energy of the tin which participates energetically in the interaction is considered (i.e. 2 mm deep), the conversion ratio is .37%. These low conversion ratios, compared to those associated with coarse mixture interactions which are on the order of a few percent, reflect the limited surface area enhancement involved during the interaction.

4.1.3 Pressure field in the water using a potential flow model

The pressure field and associated hydrodynamic flow in the water, created by the propagating interaction, can be modeled using a mechanical analogy, suggested by Ciccarelli et al. (1991). Based on the observation that the explosion is not coupled to the leading shock wave generated by the trigger, which travels at 1500 m/s in water, the flow field may be reproduced using a simple incompressible potential flow model. The interaction region appears shaped as a wedge, traveling at a relatively constant velocity along the channel. The schematic of the model is shown in fig.19 in a frame of reference moving with the interaction zone.

Away from the wedge, the flow is assumed to be uniform, U_{∞} , becoming deflected vertically by the presence of the wedge at some distance R* ahead of it. Within this region, r < R*, the flow of water is approximated by flow over a solid wedge (inclined at ~10°), as represented by the streamlines in fig.19. The pressure distribution in the water in the vicinity of the wedge can be obtained from the potential flow solution for the flow within a sector, given by:

$$F(z) = -Uz^n (4.3)$$

which yields the associated velocity potential:

$$\phi = -Ur^{n} \cos n\theta \tag{4.4}$$

where π/n is the sector angle (170°) and r ($\sqrt{x^2 + y^2}$) is the radial distance away from the apex of the wedge.

The solution for the potential flow within a sector yields unbounded velocity far from the vertex of the sector. The region of interest for the pressure field is that within R^* , which may be estimated based on the experimental pressure traces. Using the characteristic rise time of 1 ms and propagation velocity of 40 m/s yields $R^* = 4$ cm. Beyond R^* , the flow is assumed uniform, U_{∞} . Using this boundary condition as well as $P = P_{\infty}$ at $r = R^*$, the pressure field may be calculated according to the steady state Bernoulli equation. The resulting pressure distribution is:

$$P(r) - P_{\infty} = \frac{\rho U_{\infty}^{2}}{2} \left[1 - \left(\frac{r}{R^{+}} \right)^{2(n-1)} \right]$$
 (4.5)

The wedge analogy models the leading edge of the interaction as a point whereas, in reality, it is a region of finite size. Therefore the model does not reasonably represent the flow along the stagnation streamline, at this location. The pressure variation away from the apex of the wedge is shown in fig.20 at a height y = 1 cm above the tin layer, corresponding to the location of the pressure transducers. The shape of the pressure profile is similar to that recorded experimentally although yields a lower peak pressure of .12 MPa, at r = 1 cm.

4.1.4 Effect of inertial constraint

The role of the inertial confinement on the interaction was investigated by varying the height of the water overlying the tin layer. The impulse values for various water heights, calculated from the pressure profiles, are given in fig.4. As the water height or inertial constraint of the system is increased, the strength of the impulse produced in the water rises. The reason behind this trend is that the slower decay of the vapor pressure creates a stronger impulse (larger pulse width). Since this expansion drives the flow of water ahead of the interaction front, a correspondingly stronger pressure field is produced in the water. At a water height of 12 cm, a sustainer propagating interaction was always observed. However, at a water height of 5 cm, the impulse produced was insufficient to sustain the vapor film collapse process, and the interaction failed. The rapid pressure decay shown in fig.21 illustrates the failure of the propagation at a water height of 5 cm.

4.2 One-dimensional vapor expansion model

In order for the vapor film collapse process to be sustained, the impulse imparted to the water must be sufficiently strong. The expansion of the vapor provides the driving force for the hydrodynamic flow in the water, and as seen above, is influenced by the boundary conditions which determine the inertial constraint of the system. One of the factors which might contribute to the failure of propagation at the lower water height in the narrow channel

is the rate of the pressure decay in the expansion zone. If the vapor expands too rapidly (i.e. the pressure decays sharply) a corresponding weaker impulse, determined by $\int Pdt$, is imparted to the water. The expansion zone behind the leading edge of the propagating interaction is a complex, multi-phase mixture. The modeling of the expansion process is certainly complex, however, using a simple one-dimensional model of the expanding vapor, the effect of the inertial constraint on the dynamics of the expansion may be illustrated.

4.2.1 Model description

The model consists of a one-dimensional slug of water accelerated by a volume of high pressure vapor, as shown in fig.22. The motion of the interface separating the water and the vapor is governed by two equations: the conservation of energy within the vapor and the application of Newton's first law to the water mass. The time derivative of the conservation of energy equation gives:

$$\frac{d\mathbf{U}}{dt} = \dot{\mathbf{Q}} - \dot{\mathbf{W}} = \dot{\mathbf{Q}} - \mathbf{P}\frac{d\mathbf{V}}{dt} \tag{4.6}$$

where U is the internal energy, Q the heat flux and PdV the work done by the system. Assuming ideal gas behavior the internal energy may be written in terms of the vapor pressure, P, and volume, V, as:

$$\mathbf{U} = \frac{\mathbf{P} \ \mathbf{V}}{\mathbf{\gamma} - 1} = \frac{\mathbf{P} \ \mathbf{A} \ \mathbf{Y}}{\mathbf{\gamma} - 1} \tag{4.7}$$

where A is the surface area of the interface, Y is the vertical displacement of the interface (starting from some initial height Y_0) and γ is the perfect gas constant. Substituting these variables and simplifying the equation gives:

$$\frac{dP}{dt} = \frac{\gamma - 1}{AY} \dot{Q} - \frac{P \gamma}{Y} Y \tag{4.8}$$

The acceleration of the slug of water is described by:

$$\frac{d^2Y}{dt^2} = \frac{P - P_{\infty}}{\rho H_w} - g \tag{4.9}$$

where P_{∞} is the ambient pressure, ρ is the water density, H_{w} the height of the water column and g the gravitational acceleration.

The value for γ was chosen based on the results simulating the bubble vapor expansion surrounding a molten tin drop in water, which best matched the experimental observations (Ciccarelli, 1992). A value of 1.09 produced the most accurate results for the tin/water system and therefore is used here. Equations 4.8 and 4.9, non-linear of the second order, were solved by numerical integration using the Gear method.

4.2.2 Results of the effect of inertial confinement

The vapor expansion behavior was investigated under different degrees of inertial confinement, determined by the height of the overlying water. The initial conditions assume that a thin layer of water is superheated over a characteristic time period to a saturation temperature of 300° C, corresponding to a pressure of 8.6 MPa. This thin vapor layer, of initial volume AY₀, is then allowed to expand, neglecting condensation effects. The duration of the heat transfer process is not known but can be estimated from experiments based on the time between triggering and the start of the vapor expansion. In the case of a tin drop in water this time is in the order of 80 μ s (Ciccarelli, 1992). Assuming half this time is allotted to collapsing the vapor film, the time for heat transfer is ~40 μ s. This gives an initial vapor film thickness of ~50 μ m.

Recall that propagations in the narrow channel occurred consistently at a water height of 12 cm, and always failed at a height of 5 cm. The vapor expansion dynamics were evaluated at heights of 1, 5 and 12 cm and the pressure variation with time is presented in fig.23. As seen the vapor expands very rapidly during the first ~0.2 ms, slowing down as the interface approaches the maximum height. At this point, the vapor is overexpanded at a pressure of about .011 MPa, causing it to collapse. Under a lower water height (lower inertia), the vapor expands more rapidly, attaining its minimum pressure in ~.1 ms, for a water height of 1 cm, compared to ~0.35 ms for a height of 12 cm. These results illustrate that the inertial constraint alone of the one-dimensional propagation in the narrow channel significantly alters the expansion behavior of the vapor, which affects the impulse, or the strength of the disturbance communicated to the adjacent, stable vapor film.

4.3 Perturbation of the interaction front

The sustained spatial propagation of the interaction is achieved by an effective transmission of the disturbance generated by the expanding vapor, through the water, to the mixture ahead of the interaction front. In the highly confined narrow channel (with adequate vertical confinement), the propagating interaction was consistently sustained. In order to acquire a broader understanding of the characteristics of this propagating interaction, an experiment was performed to test the behavior of the interaction when subjected to a sudden perturbation, created by the abrupt transition from the narrow channel (1.25 cm) to the wider one (5 cm). As the explosion front approaches the transition, the change in geometry affects the pressure field in the water (divergence of the flow) and interferes with the transmission of the pressure disturbance, before the interaction front reaches this location. When the interaction front passes the transition point, the sideways expansion also introduces a curvature of the front. The additional expansion causes a sharper decay of the pressure in the water, resulting in a weaker impulse which is unable to sustain the vapor film collapse process. As observed, the propagation consistently fails under these conditions. The curvature effect on the pressure decay rate may be illustrated by comparing the pressure fields generated in the water ahead of a planar and curved front, as shown in fig.24. The potential flow model for the flow over a wedge can be used to calculate the pressure field along the stagnation streamline in the case of a planar front moving at 40 m/s, as described in section 4.1. The effect of the sudden expansion when the interaction transits into the larger channel may be represented by the pressure field generated by an expanding sphere, which decays inversely with distance from the sphere. A sphere diameter of 1 cm is chosen to simulate the curvature of the front when it emerges from the narrow channel, corresponding to a distance of .5 cm ahead of the wedge. The comparison of the two pressure distributions is illustrated in fig.25. The pressure in the water ahead of the front drops more rapidly with distance away from the sphere, causing a decrease in the strength of the impulse, apparently below the critical value required to sustain the vapor film collapse process.

Another factor which can promote the failure of the interaction when suddenly perturbed is the stability of the interaction front itself. If the interaction front is unstable, the perturbation induced by the sudden lateral expansion could promote its breakdown, due to the growth of irregularities in the form of local curvatures across its span. The decay of the propagating interaction depends on the evolution of the irregularities (or instabilities) of the front, i.e. whether the boundary conditions permit their growth or suppress them. To

independently test the stability of an interaction front an appropriate experiment would consist of initiating a propagating interaction in channels of various widths, and determine if there is some critical channel width for which the propagation breaks down. Presumably, in a channel of critical width, the wavelength associated with the unstable mode would be shorter than the width of the channel, and therefore could be sustained. In a narrower channel this wavelength would be suppressed.

A possible source of instability of the interaction front is related to the boiling dynamics of the steady state film boiling regime, which creates variations in the vapor film thickness over the surface area of the melt. During this period, vapor bubbles are constantly growing and "pinching off" as they become too large and condense out, producing a constantly fluctuating, wavy vapor layer. When the interaction front passes over this interface, there will be local differences in the vapor film collapse time and perhaps only partial collapse in some areas. Consequently, the pressure front becomes non-uniform. A non-uniform front implies lateral pressure gradients and thus local curvatures of the front. The curvature effects weaken the pressure field in the water further reducing the effectiveness of the vapor film collapse process. The resulting loss in coherence of the energy release promotes the breakdown of the interaction front.

4.4 Effect of the unconfined condition in the cylinder on the characteristics of the interaction

4.4.1 Initiation of a propagating interaction

The characteristic effect of the unconfined condition on the initiation of an interaction in a stratified configuration was the unpredictable behavior of the system: under similar initial conditions propagating interactions ranging in energetic intensity and no interactions at all were observed. Such initiation problems have plagued other intermediate/large scale vapor explosion studies (e.g. Sainson et al., 1993; Anderson et al., 1988), which resulted in a similar erratic response to the trigger. In all cases, one liquid is poured into the other and allowed to settle to form a stratified layer, however, it is quite conceivable that the initial interface conditions vary from one trial to another. In fact, as Sainson et al. have noted, if there is some pre-mixing at the interface between the two liquids the initiation of a

propagating interaction is more probable. The reason resides in the fact that the pre-mixing of the liquids presents a larger surface area, such that, following the collapse of the vapor film by the triggering shock wave, a greater amount of heat can be transferred to the water, creating a more energetic initial disturbance.

The inconsistent behavior in the present case was noticed to originate during the triggering stage. The shock wave generated by the trigger collapses the vapor film over a finite area and forces the two liquids into contact. From the evidence exhibited on the high speed films, there is a sudden generation of vapor which, however, does not initiate a propagating interaction. Rather, this initial disturbance grows, during the next few ms, through subsequent vapor bubble growths and collapses in the vicinity of the trigger. Then either a larger disturbance travels radially outward or the initial disturbance decays without effect. Possibly, the observed interaction which travels radially outward is not a "sustained" propagation, but rather an overdriven interaction resulting from the violent collapse of the vapor bubbles produced immediately following the triggering. The thrust of the collapse could generate a disturbance over a larger surface area of the tin, resulting in the collapse of the vapor film and more vapor production. However, there is no propagation mechanism to sustain the interaction over the entire surface area, therefore the interaction is spatially limited.

One of the reasons preventing the initiation of a propagating interaction in the cylindrical geometry is the global curvature of the interaction front. The effect of this curvature on the pressure field generated in the water, ahead of the explosion front, may be illustrated using a potential flow model. The spatial growth of the interaction in the cylindrical geometry appears as a flattened cone expanding in the radial direction. The associated flow field is not conveniently described, however, the characteristic feature, the divergence effect created by the radial expansion, may be exposed by considering the flow field produced by a cylinder expanding in the radial direction. The potential flow for the cylindrical model, as depicted in fig.26, is given by:

$$\phi = R\dot{R} \ln \frac{r}{R} \tag{4.10}$$

where R is the radius of the cylinder, \dot{R} is the radial propagation velocity and r the radial distance away from the cylinder surface. Similarly to the wedge model the solution for the potential flow outside the cylinder yields unbounded velocity far away from the surface of

the cylinder. Unlike the flow in the channel, the divergence effect creates an unsteady flow. Therefore it is not possible to determine a characteristic distance, R*, away from the leading edge (cylinder surface) within which the streamlines are affected, and outside of which the velocity is uniform. Such a distance changes with the radial position R of the cylinder.

Using the unsteady Bernoulli equation:

$$\frac{P}{\rho} + \frac{1}{2} (\nabla \phi)^2 + \frac{d\phi}{dt} = constant$$
 (4.11)

and the boundary condition $P = P_S$ (stagnation pressure) at r = R, the following equation for the pressure distribution in the water is obtained:

$$P(r) = P_{s} - \rho R^{2} \left| \frac{1}{2} \left(\frac{R}{r} \right)^{2} + \ln \frac{r}{R} - \frac{1}{2} \right|$$
 (4.12)

Compared to the pressure distribution associated with the wedge model, it is seen that the divergence effect of the flow introduces another parameter, the radius of the expanding cylinder (R), into the equation governing the pressure decay ahead of the cylinder. For the purpose of comparison with the pressure distribution created by a planar front, described by the wedge model, the imposed boundary condition is that the pressure at r = 1 cm matches that of the wedge model at the same location (0.12MPa). The pressure distributions are presented in fig.27, for the wedge and cylinders of various radii, R, both moving at 40 m/s. The rate of pressure decay in the water depends on the radial position, R, of the cylinder: the decay is sharper at small radii, corresponding to the stronger effect of curvature or divergence of the flow. As R increases the front begins to resemble a planar wave, thus accounting for the reduction in the rate of pressure decay ahead of it. The comparison of the pressure fields generated by the wedge and the cylinder illustrates the relative effect of the curvature of the front on the rate of the pressure decay. The essential feature is that curvature of the front weakens the flow field, especially at the smaller radii. The observed initiation difficulties and inability for a sustained propagation to develop therefore can be attributed to this effect.

On more speculative grounds, the erratic behavior of the interactions could also be the result of an unstable phenomenon, associated with the propagation of the explosion front. As mentioned in section 4.3, an unstable interaction front is sensitive to the boundary conditions which determine whether a perturbation grows or decays. In the unconfined condition of the cylindrical tank, irregularities in the shape of the front, or instabilities, are free to develop since there are no boundaries to suppress them.

4.4.2 Energetics

The mechanisms involved in the propagation of a stratified vapor explosion are inherently difficult to identify because they occur on a very short time scale. In order to discern the effect of the boundary conditions on the interaction, it is useful to turn to the energetics associated with the event. The energy yield of the interaction was evaluated in the manner presented in section 4.1, based on the impulse values calculated from the pressure records. The yield/surface area is given in Table 2, including the yield/surface area for the stratified water/tin propagating interaction in the narrow channel and a single tin drop explosion in water (Ciccarelli, 1992).

The energy yield for the 0.5 g drop is less than twice as large than for the 4 kg stratified tin layer. The difference in initial surface area over which the interaction occurs is about three orders of magnitude. This suggests that the dynamic processes following the collapse of the vapor film (mixing, rapid heat transfer and vaporization) occur at a similar rate in both cases. Considering also that the yield/surface area results of the drop, narrow channel and cylindrical tank are of the same order of magnitude, it seems that the boundary conditions of the system do not influence the energetics of the interaction significantly.

An estimate of the amount of tin which participates energetically in the interaction was made based on the tin fragments collected following an interaction. Again, fragments smaller than 1 mm in size were considered to form the effective mixing depth of the interaction. The values for the cylindrical tank and the narrow channel are also given in Table 2. The yield/surface area ratio of the narrow channel and cylindrical tank are roughly the same although the estimated effective mixing depth is more than twice as large in the channel than in the cylindrical tank. This is probably a consequence of the greater degree of confinement in the channel, resulting in larger vapor velocities in the wake of the interaction region. The tin is further fragmented in this zone due to the hydrodynamic shearing action but loses its heat slowly such that it doesn't contribute to the energetics of the event. The conversion ratio, calculated based on the amount of tin which participates energetically in the interaction (i.e. ~0.86 m.n deep), is 0.26%.

In contrast to the energetic explosion in a coarse mixture of melt fragments in coolant, the interaction in the stratified configuration results in a less coherent release of energy, due to the significantly smaller surface area available and the little fragmentation involved during the interaction. This was clearly observed in the experiments where there were two interactions. The second one, traveling through the mixture of lofted tin fragments, water and steam, was much more violent (higher over pressures and propagation velocities) than the first and produced considerably finer fragmentation of the tin. In this context, the first interaction can be described as a "precursor" event, creating the appropriate conditions for a second more energetic interaction.

5.0 CONCLUSIONS

The characteristics of a propagating interaction through a stratified tin/water mixture in a narrow channel were previously reported by Ciccarelli et al. (1991). Their study showed that sufficient inertial constraint is essential to sustain a propagating interaction, provided by the height of the water above the tin layer. The effect of boundary conditions on the dynamics of the interaction was further investigated in the present study and was found to play a significant role in the self-sustained propagation of a stratified tin/water interaction.

Using a one-dimensional model of the expansion of a vapor region below a column of water, it was shown that the rate of the pressure decay in the vapor decreases with increasing water height. The slower pressure decay results in a stronger impulse, which drives the flow ahead of the leading edge of the interaction, generating the pressure and flow field in the water required to sustain the vapor film collapse process.

The outcome of a sudden lateral expansion on the interaction front in a channel was investigated experimentally. A propagating interaction was initiated at one end of a channel, formed by two sections of 1.25 and 5 cm in width. The sudden perturbation to the interaction at the sudden transition from the narrow channel to the wider one caused it to fail consistently. To illustrate the effect of curvature of the interaction front, which develops as it transits into the larger channel, the pressure decay in the water ahead of the curved interaction front was evaluated and compared to that ahead of a planar front. The pressure decays at a faster rate with distance ahead of the curved front, indicating that the additional expansion produces a weaker impulse in the water, inadequate to sustain the collapse of the vapor film.

The effect of the absence of confining walls on the explosive interaction between molten tin (4 kg) and water, in a stratified geometry, was experimentally investigated in a cylindrical tank, triggered at the center. The systems response to the trigger varied erratically, resulting in both violent interactions and no interaction at all, with almost equal frequency of occurrence. Successfully triggered events consisted of either a single or double interaction. The first interaction traveled radially outward 5 - 11 cm from the center, at 30 - 60 m/s, producing over pressures of 0.15 to 0.5 MPa. This event however was suspected to

be the result of an overdriven interaction, resulting from the violent collapse of vapor bubbles generated during the first few ms following triggering, and thus not a truly sustained propagation. This interaction often served as a "precursor" event for a second, more energetic one, initiated in the coarse mixture of water and melt fragments lofted after the passage of the first interaction. The resulting fragmentation of the tin reflected the violence of the interaction: 6% vs. 19% of the total tin mass was fragmented to particles < 1 mm in size, for the single and double interactions respectively.

The difficulties encountered in initiating a propagating interaction are related to the curvature effect created by the boundary conditions. This effect was illustrated through a comparison of the pressure distributions associated with the potential flow models for the flow over a wedge, representing a planar front, and an expanding cylinder. The divergence of the flow in the cylindrical case produces a sharper pressure decay in the water ahead of the interaction front, resulting in a weaker impulse.

Considering that fragments smaller than an arbitrary size of 1 mm participate energetically in the interaction, the thickness of the layer of tin involved in the single interaction is estimated to be 0.86 mm. The energy yield/surface area of the interaction, calculated based on the pressure impulse (JPdt) imparted to the water, is 0.30 J/cm², giving a conversion ratio of thermal to mechanical energy of 0.26%. Comparison of the yield/surface area with that of a single exploding tin drop (0.5 g) in water, and a stratified tin/water interaction in a narrow (1.25 cm wide) channel, shows that the yields are of the same order of magnitude, suggesting that the rate of the dynamic processes occurring are similar, and thus the energetic are not significantly influenced by the geometry.

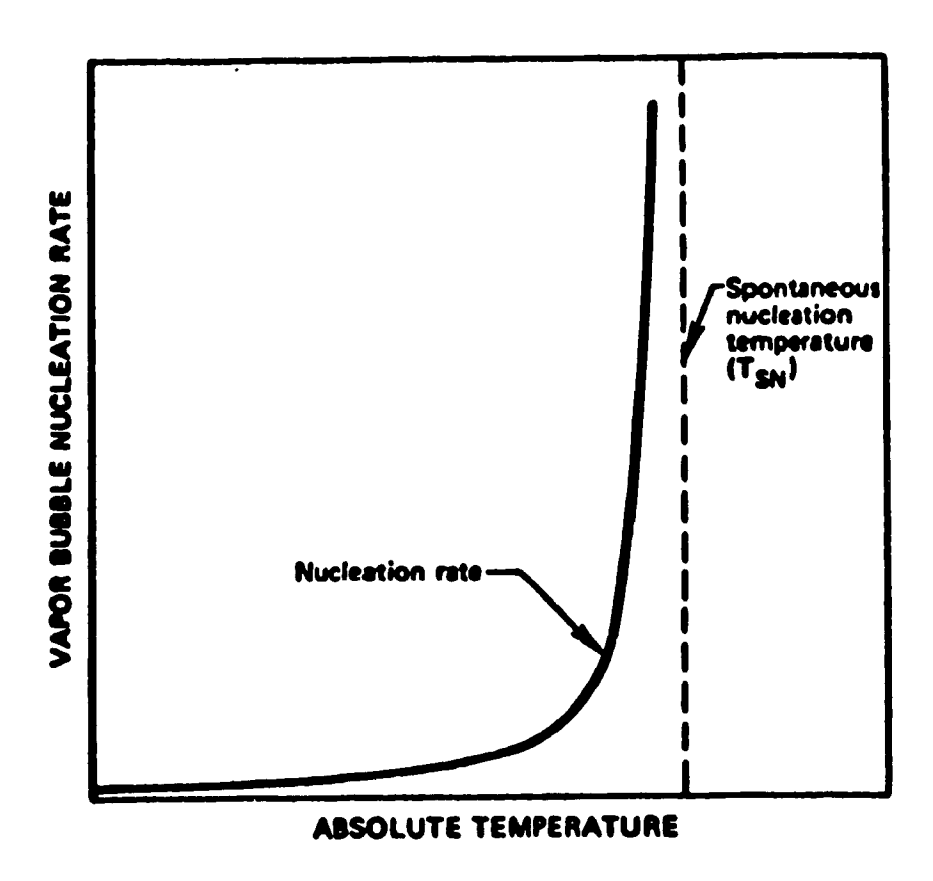


Fig. 1 Illustration of spontaneous nucleation model. (Cronenberg and Benz, 1980)

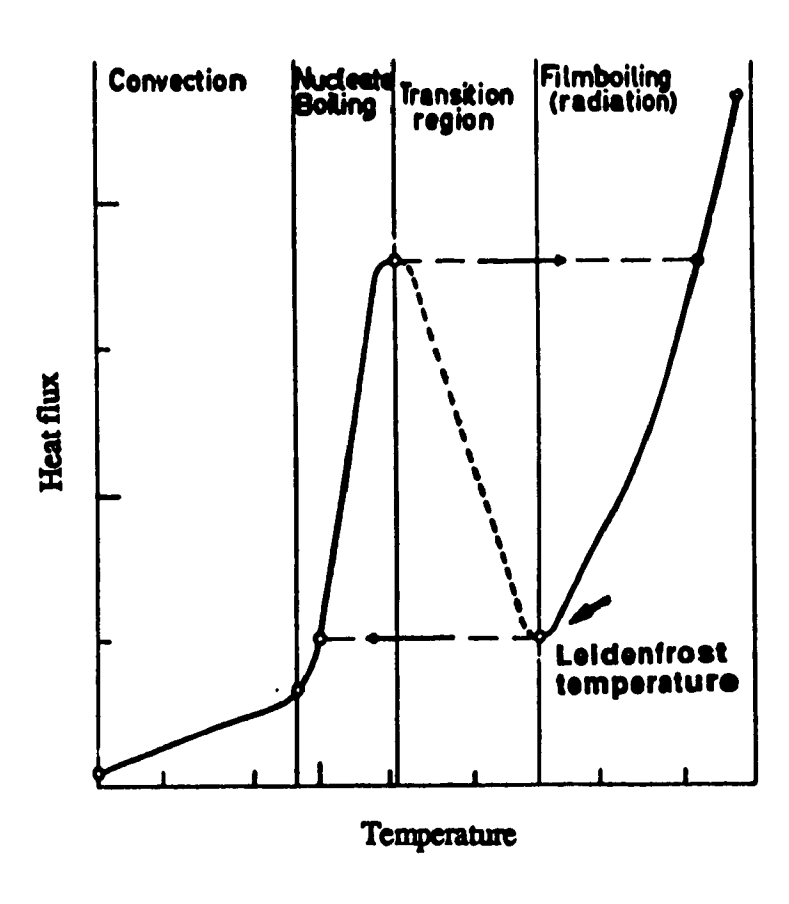


Fig.2 Boiling curve for water

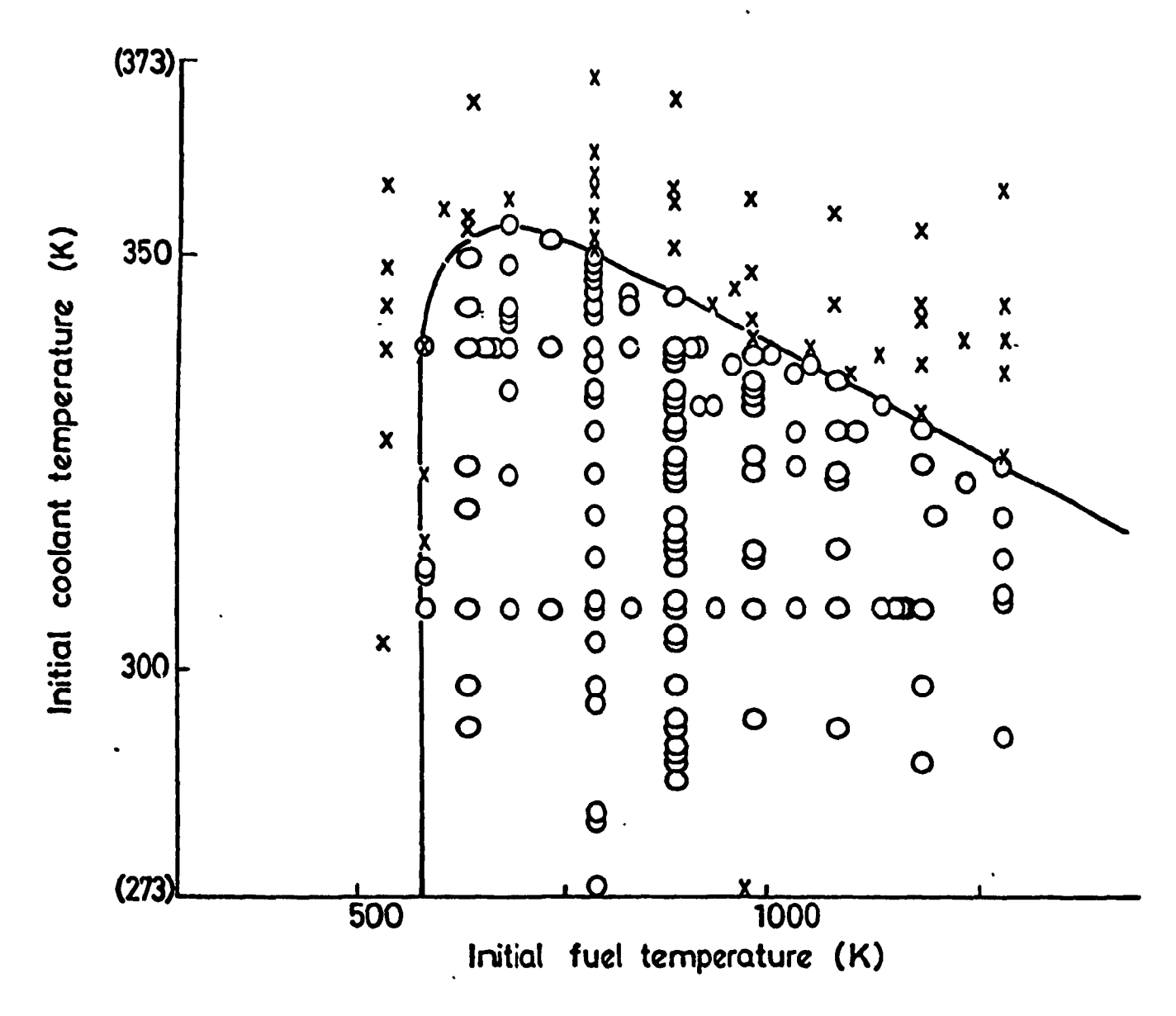


Fig.3 Fuel-coolant interaction zone for 1.2 x 10⁻² kg of tin dropped into water. (Dullforce et al., 1976)
O indicates interaction
X indicates no interaction

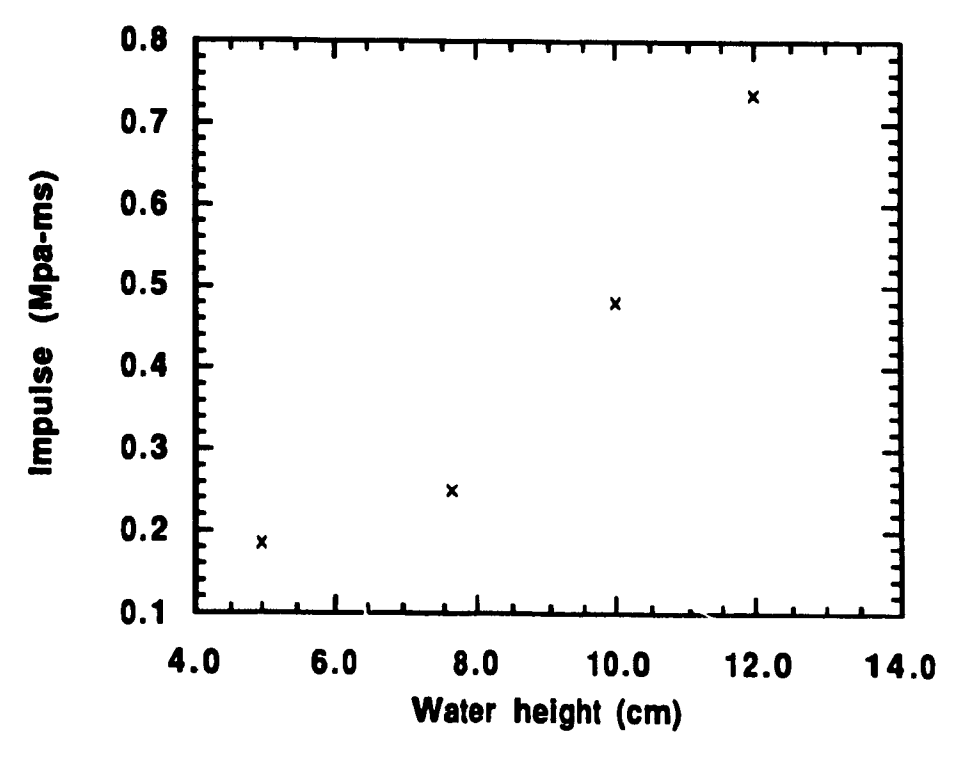


Fig.4 Pressure impulse for various water heights in narrow channel.

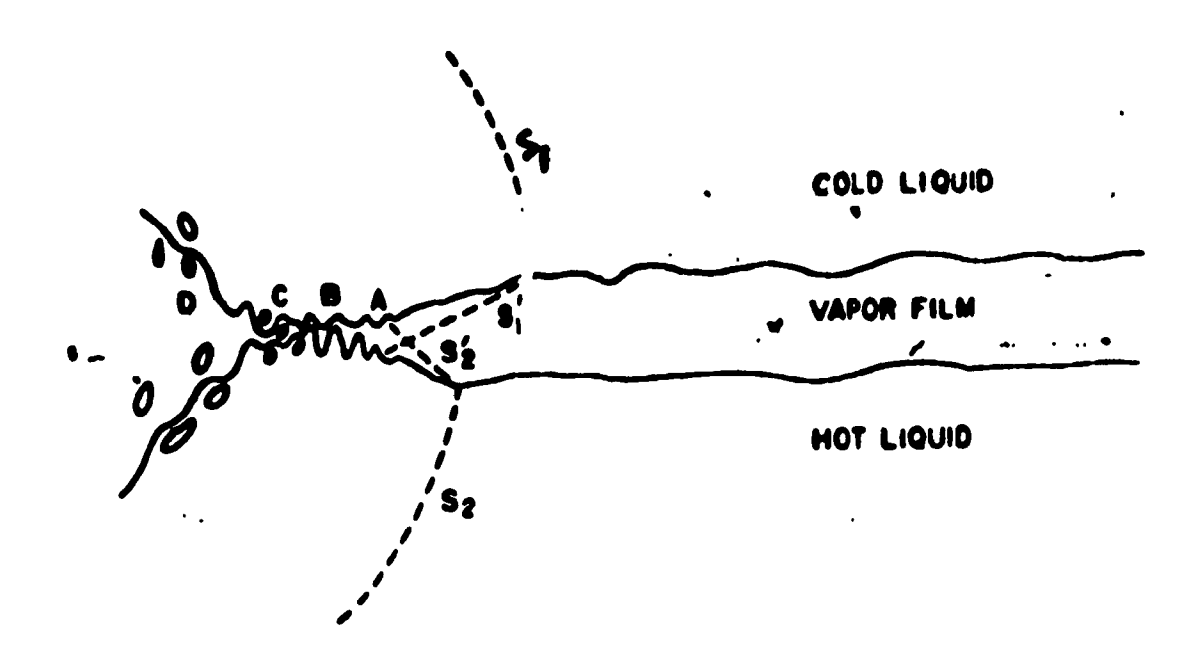


Fig. 5 Schematic of Harlow and Ruppel vapor explosion propagation model. (Harlow and Ruppel, 1981)

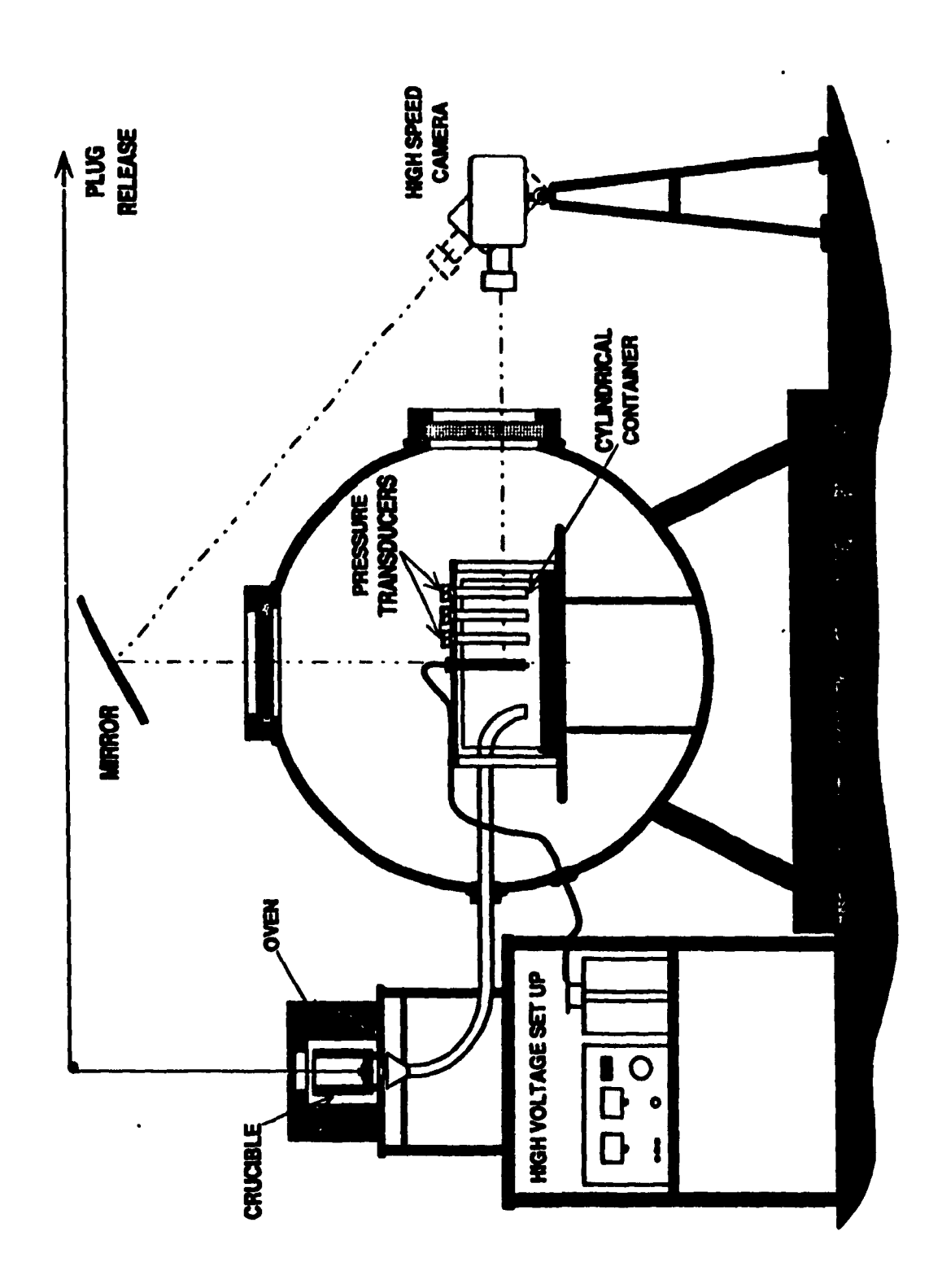


Fig.6 Schematic of experimental facility.

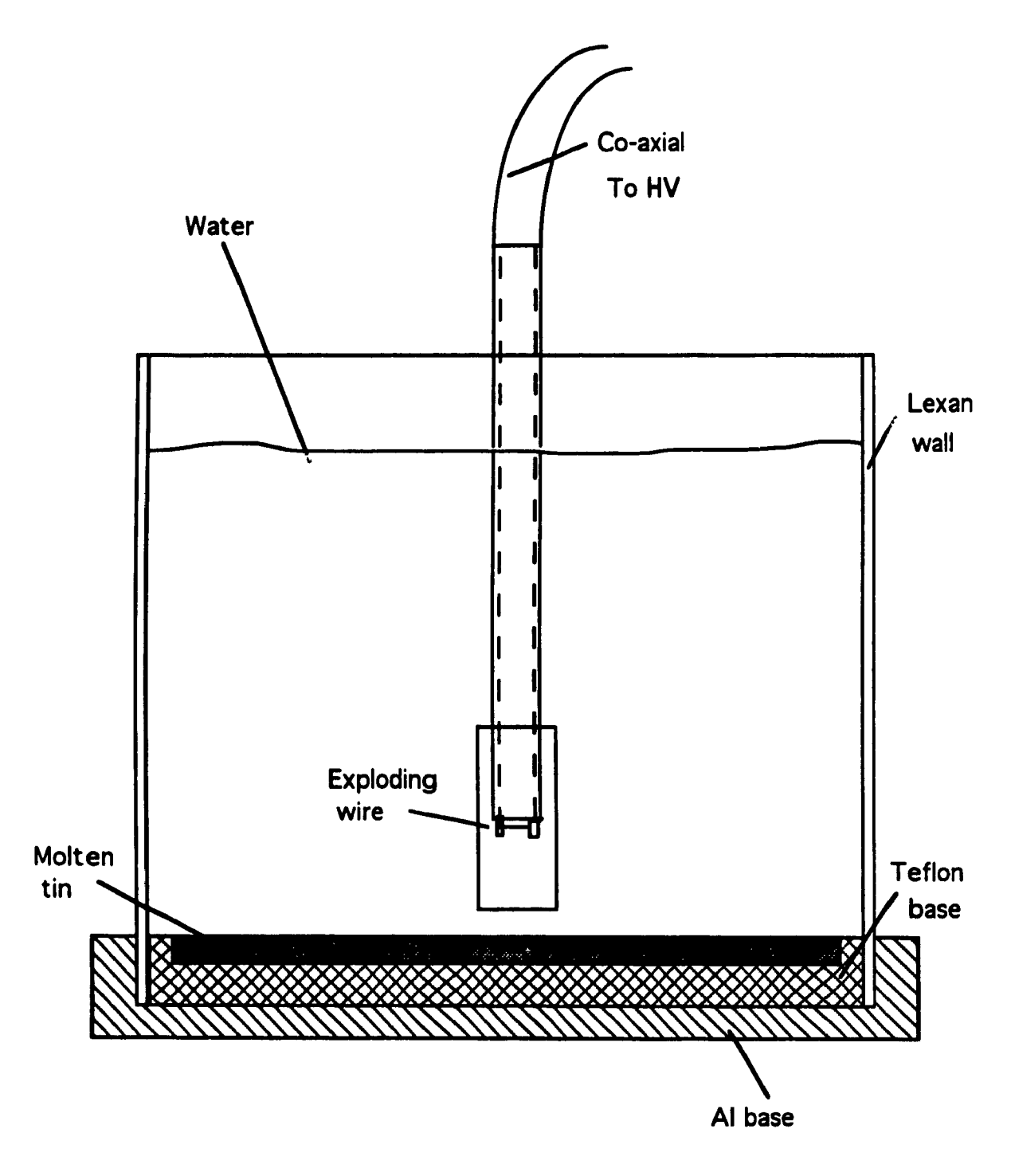


Fig.7 Schematic of cylindrical tank.

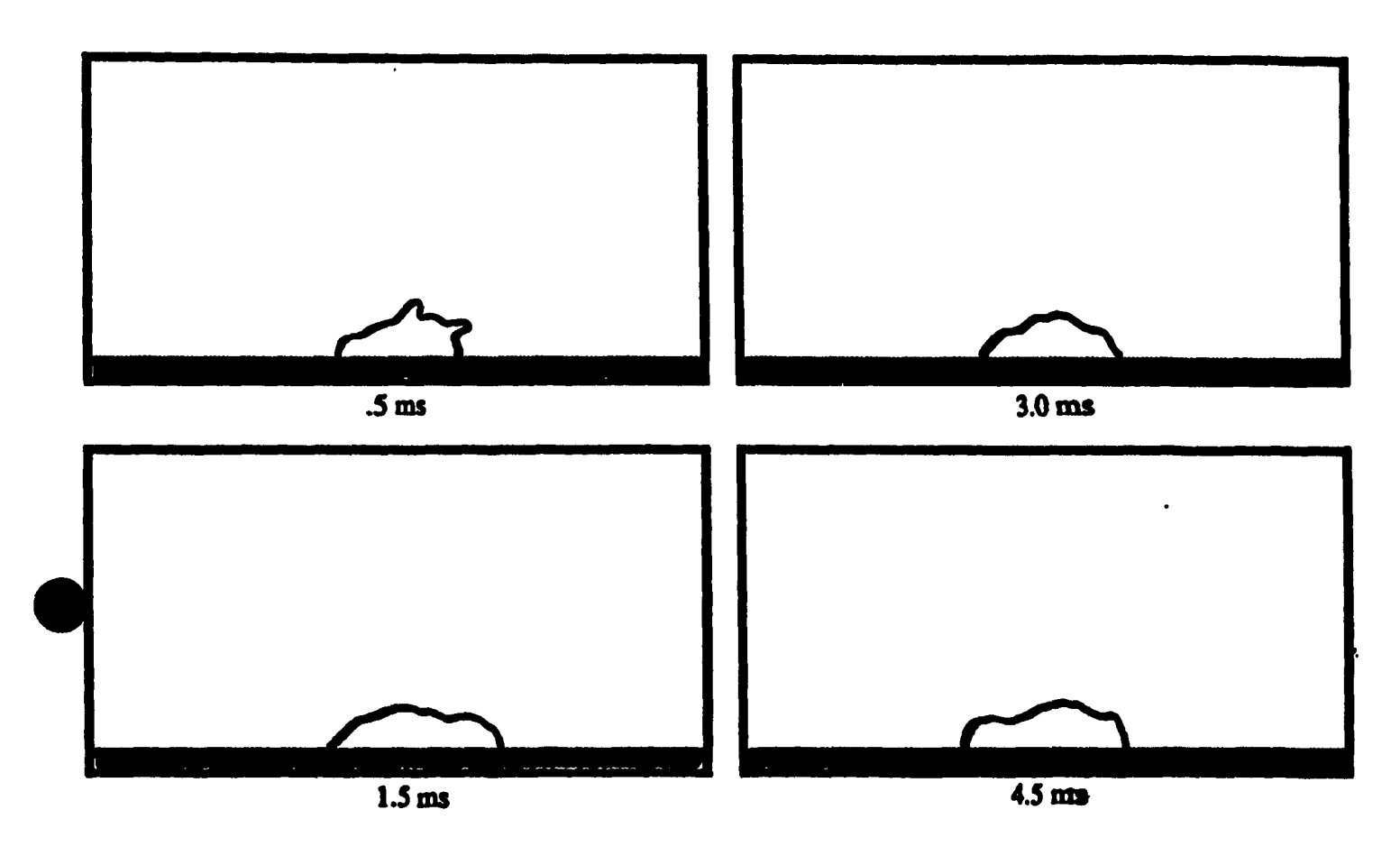


Fig.8 Illustration of the growth of the first interaction in the cylindrical geometry, from single frames of Hycam film.

Center of frame represents center of tank; scale 1:3.5.

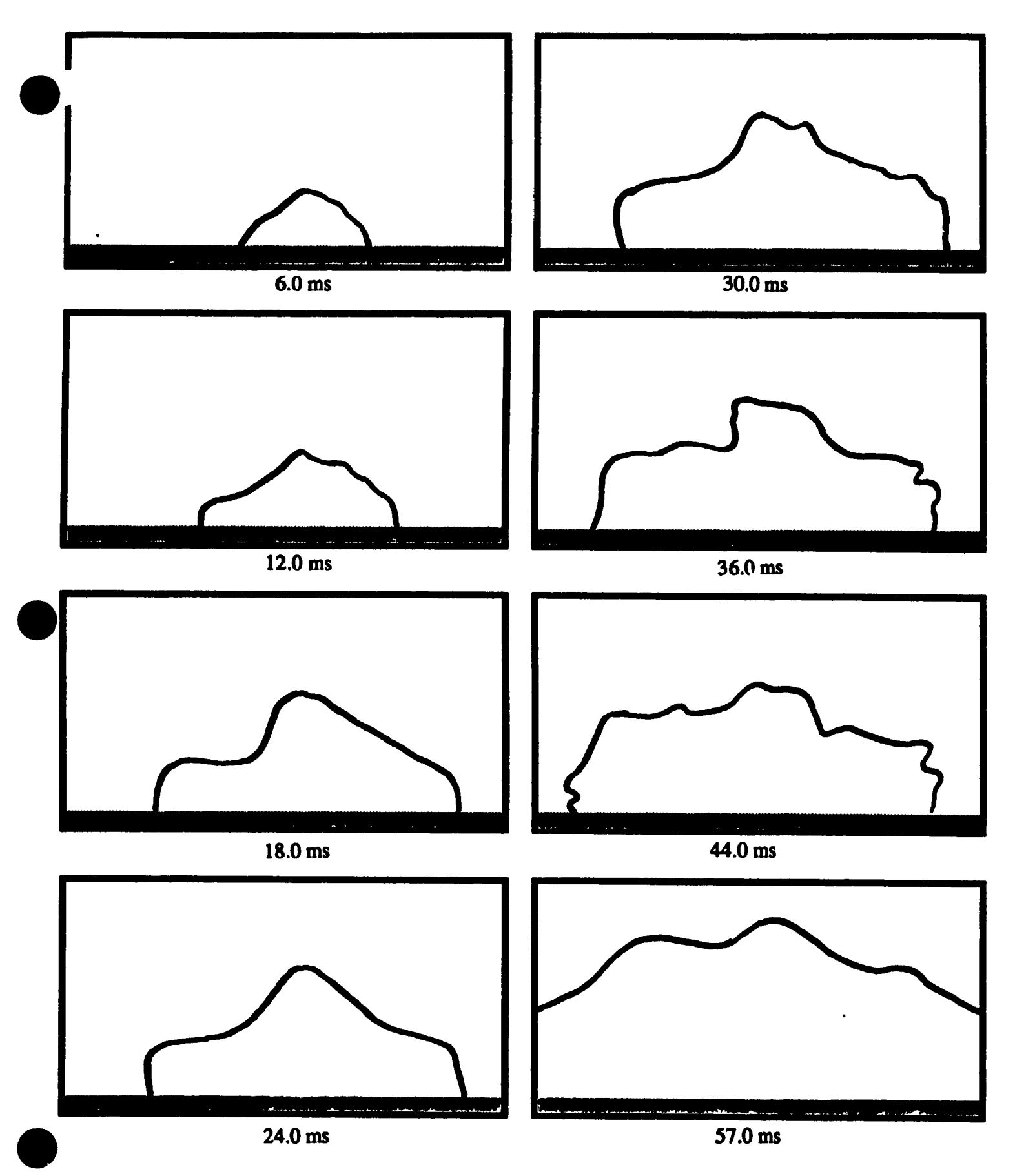


Fig.8 cont'd

Table 1 Characteristics of single interactions.

TRIAL NO.	AVERAGE VELOCITY (m/s)	OVERPRESSURES (MPa)	DEBRIS < 1 mm (% of total tin mass)
2	•	•	5.0
3	50	.2550	•
4	54	.1438	7.6
5	60	.1530	5.2
6	•	•	6.0

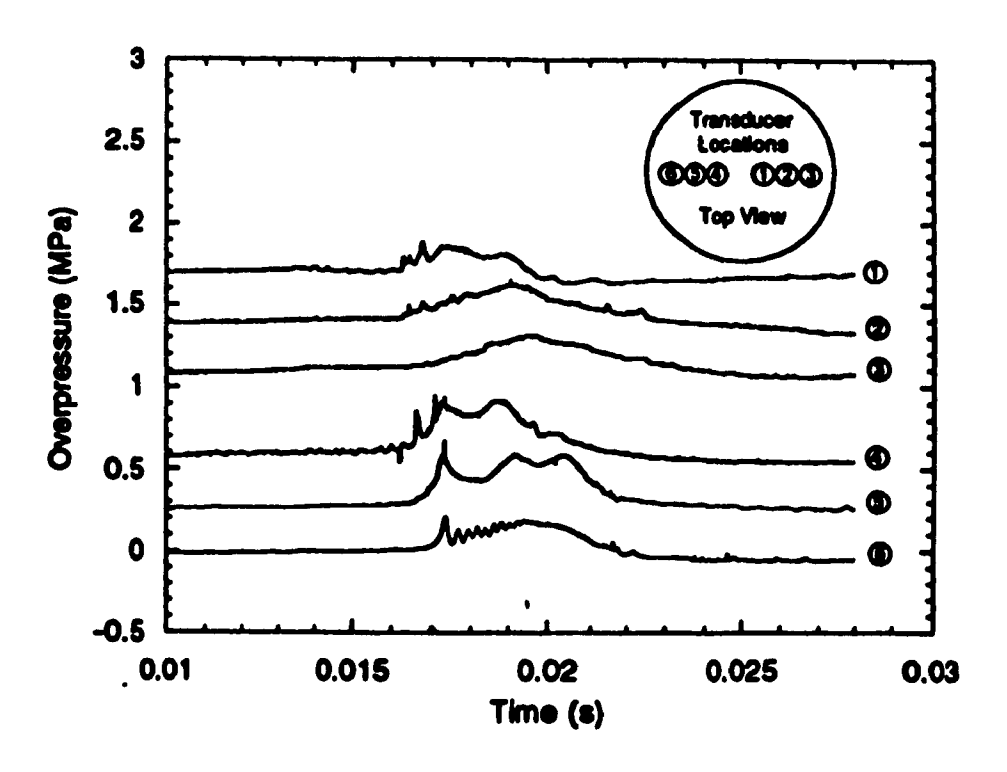


Fig.9 Pressure recorded during single interaction in cylindrical tank.

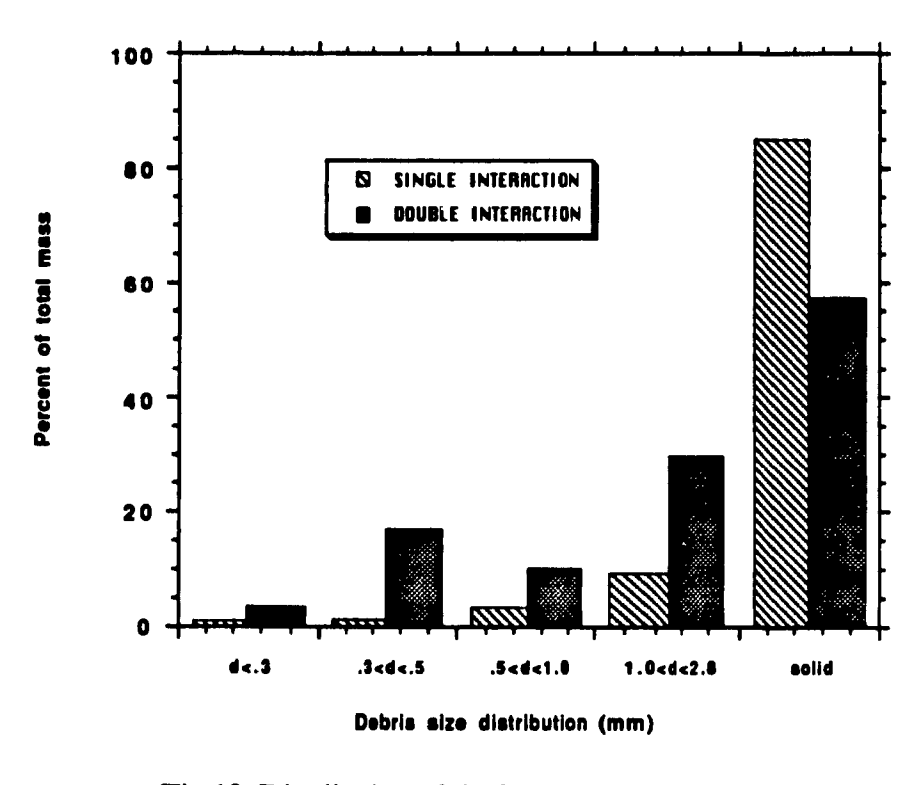


Fig. 10 Distribution of tin fragment sizes following single and double interactions.

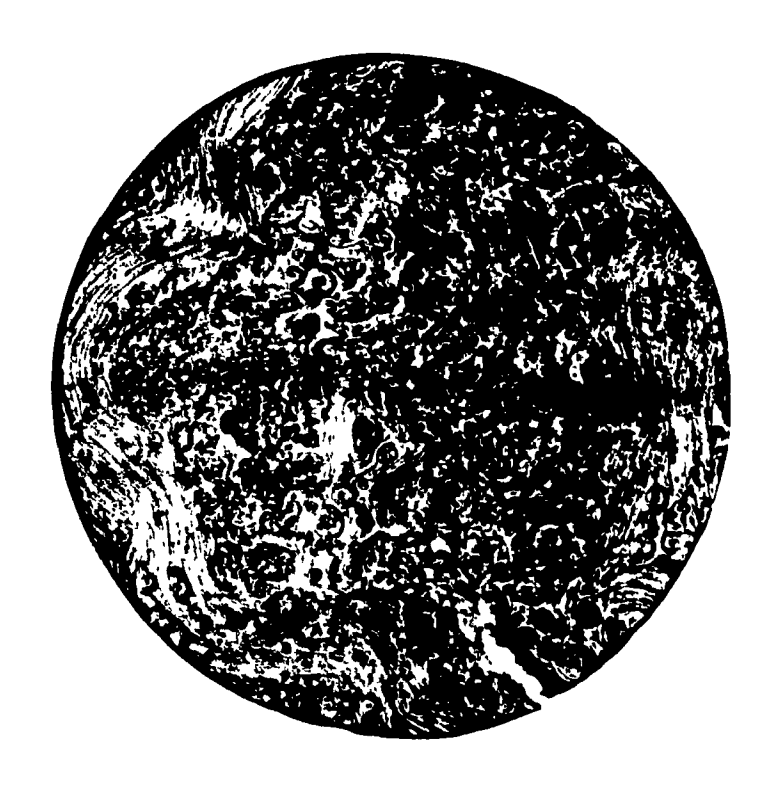


Fig.11 Photo of remaining tin disc following a single interaction. Interaction did not travel over entire surface area as shown by non-uniform dispersal of fragments.

(Line at bottom right is cut made during removal from tank.)

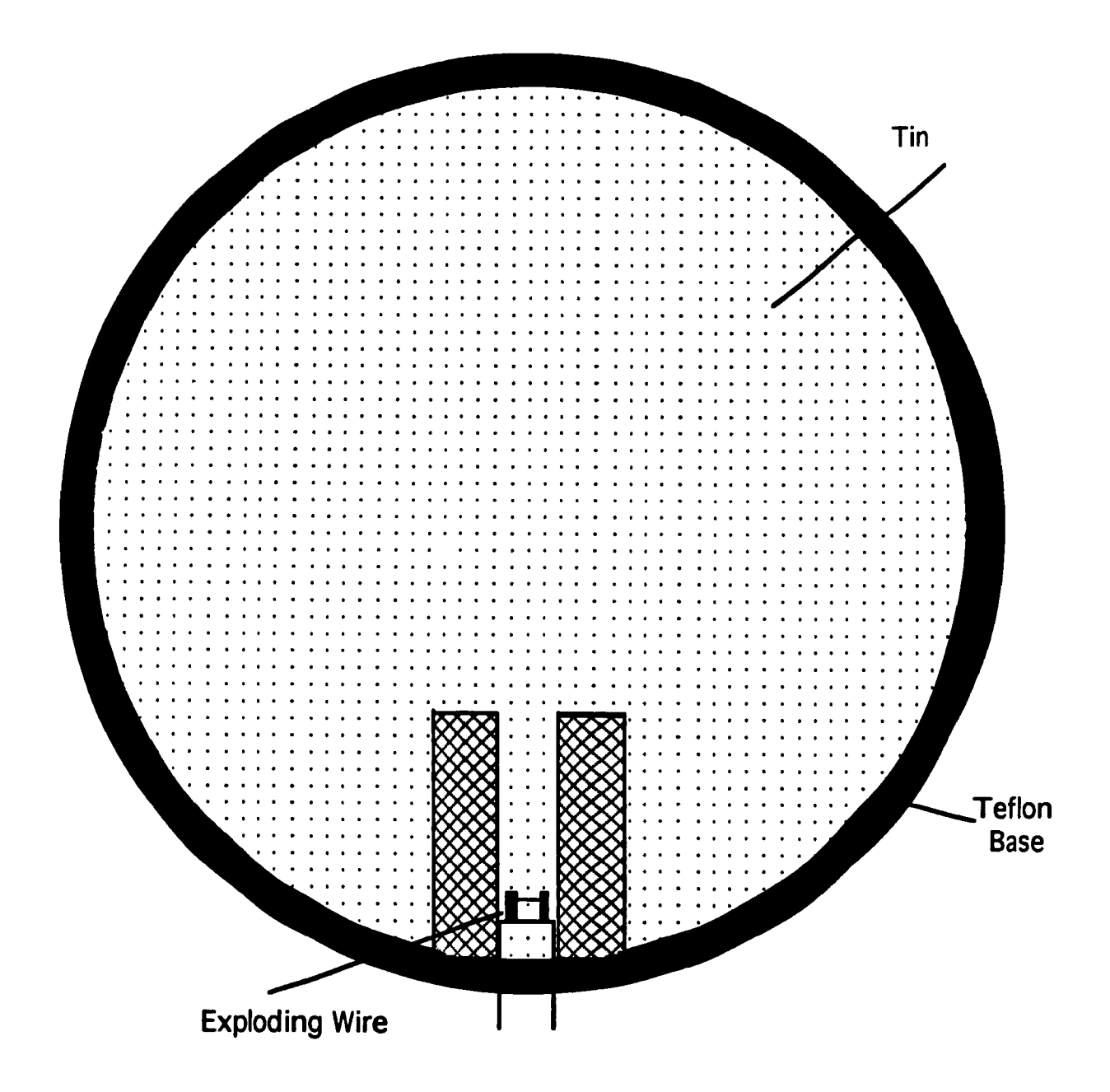


Fig.12 Schematic of narrow channel confinement in cylindrical tank.

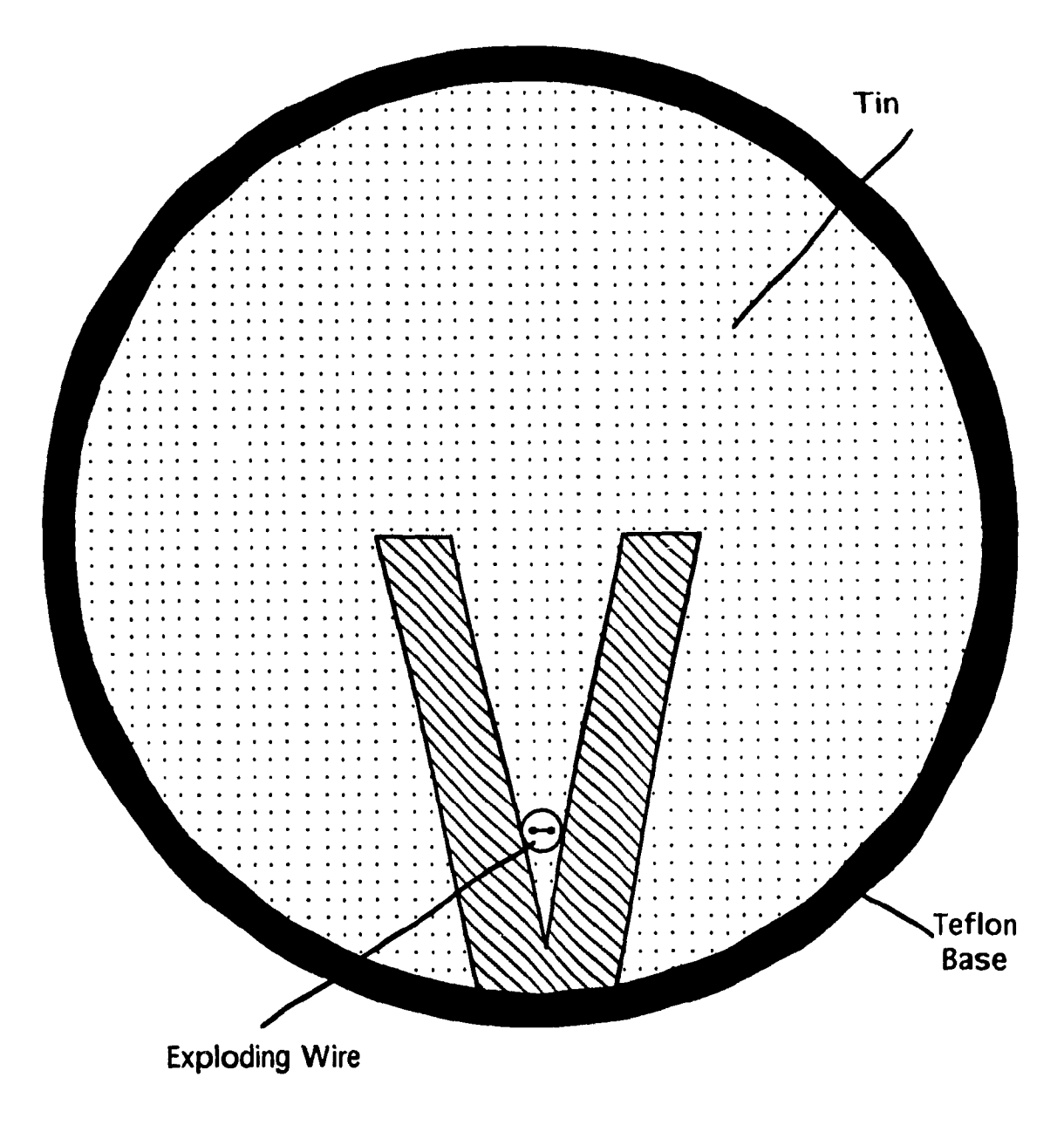


Fig. 13 Schematic of wedge shape confinement in cylindrical tank.

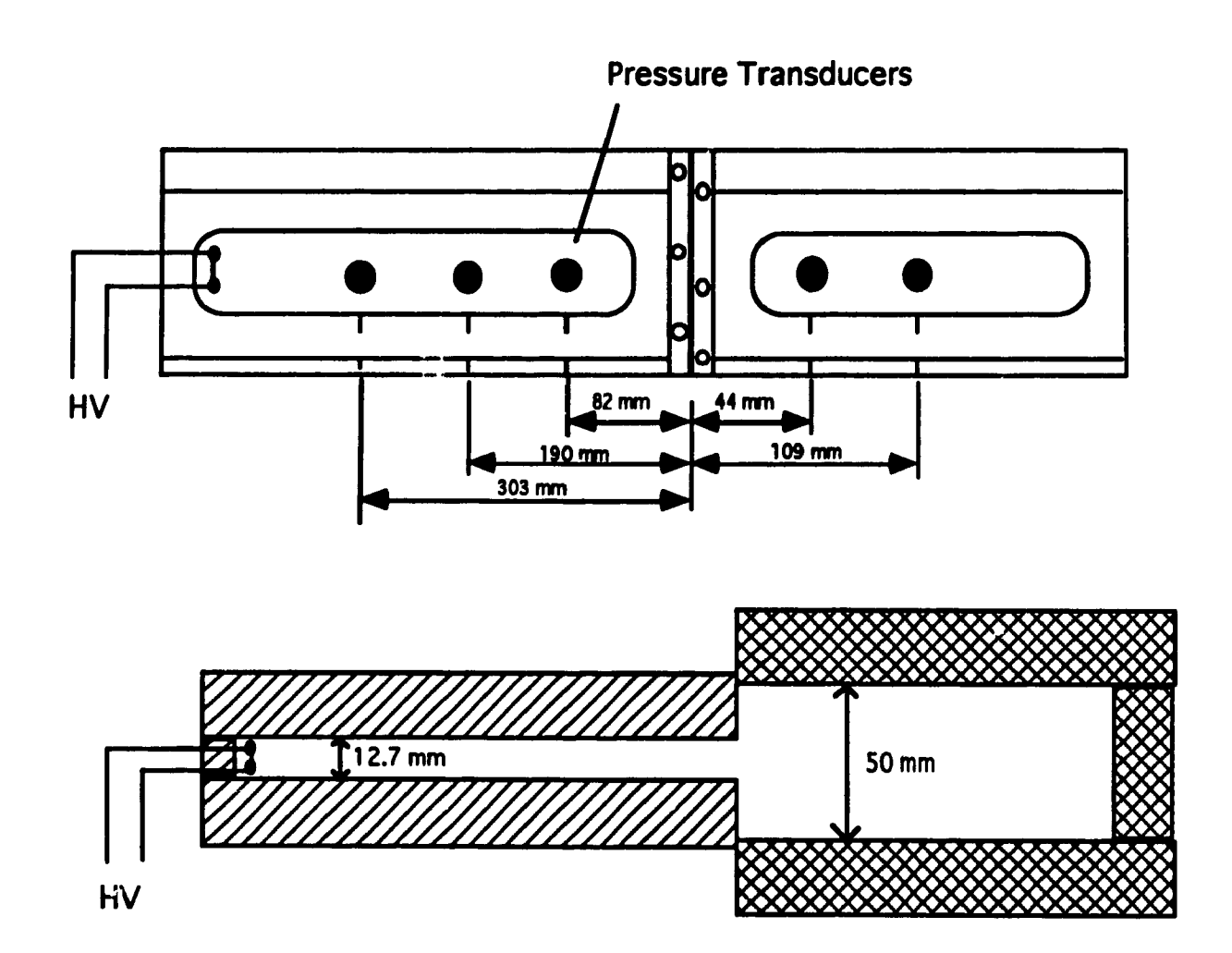


Fig.14 Schematic of double-width channel.

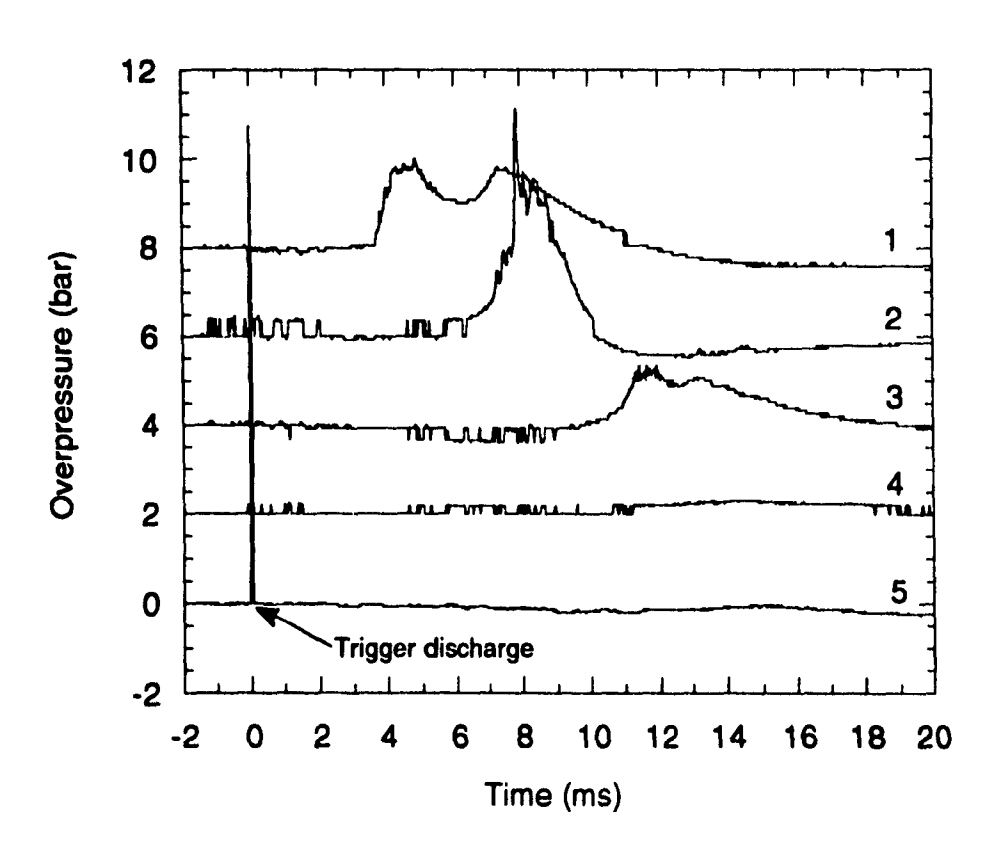


Fig.15 Pressure recorded during propagating interaction in double-width channel. Sudden expansion from 1.25 cm to 5cm, between transducers #3 and #4, results in failure of the interaction.

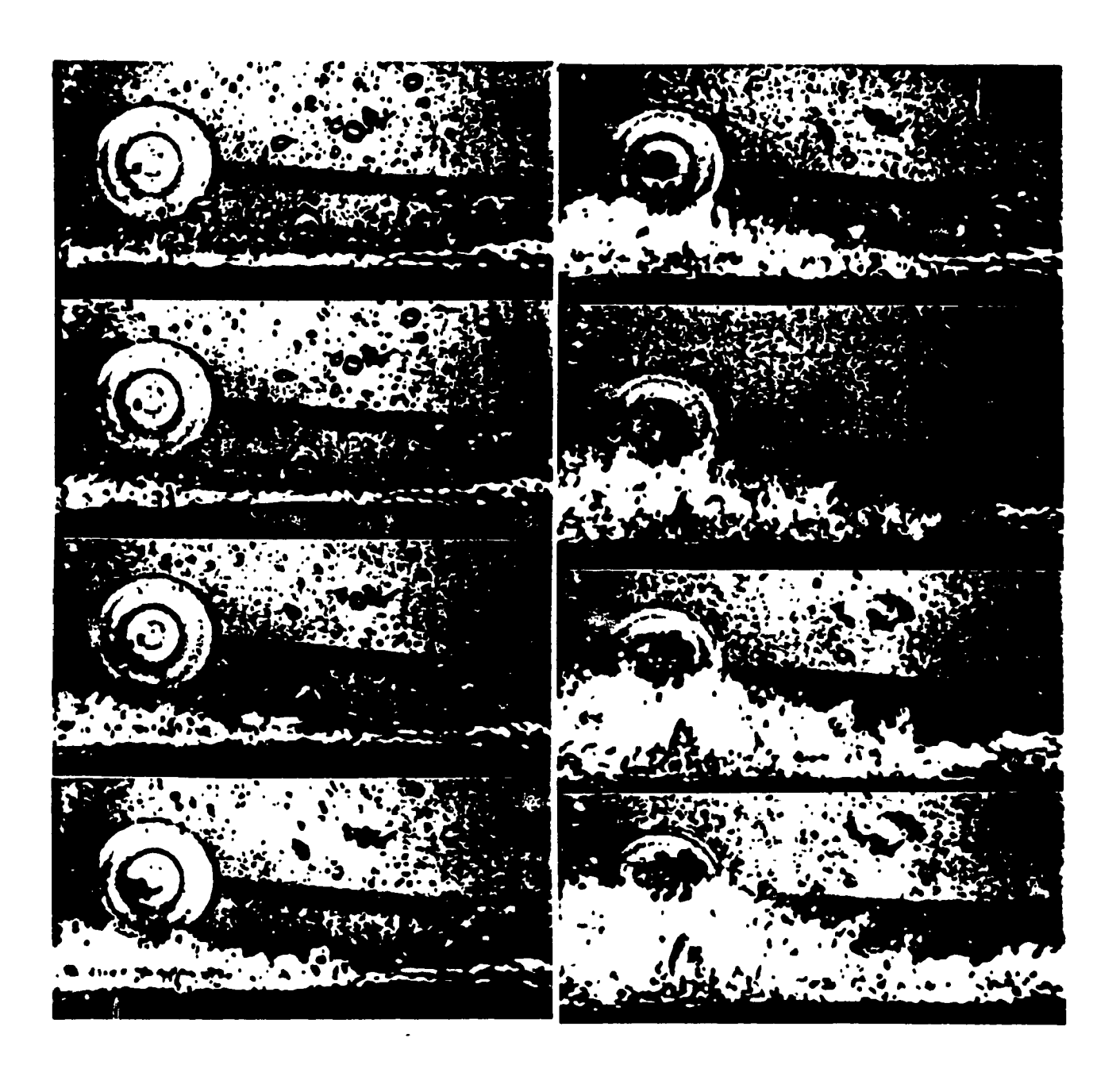


Fig. 16 Singles frames from Hycam film illustrating self-sustained propagation of interaction in stratified tin/water system. Time between frames is 400 µs. Outer diameter of transducer plug is 2.54 cm, visible at left. (Ciccarelli et al., 1991)

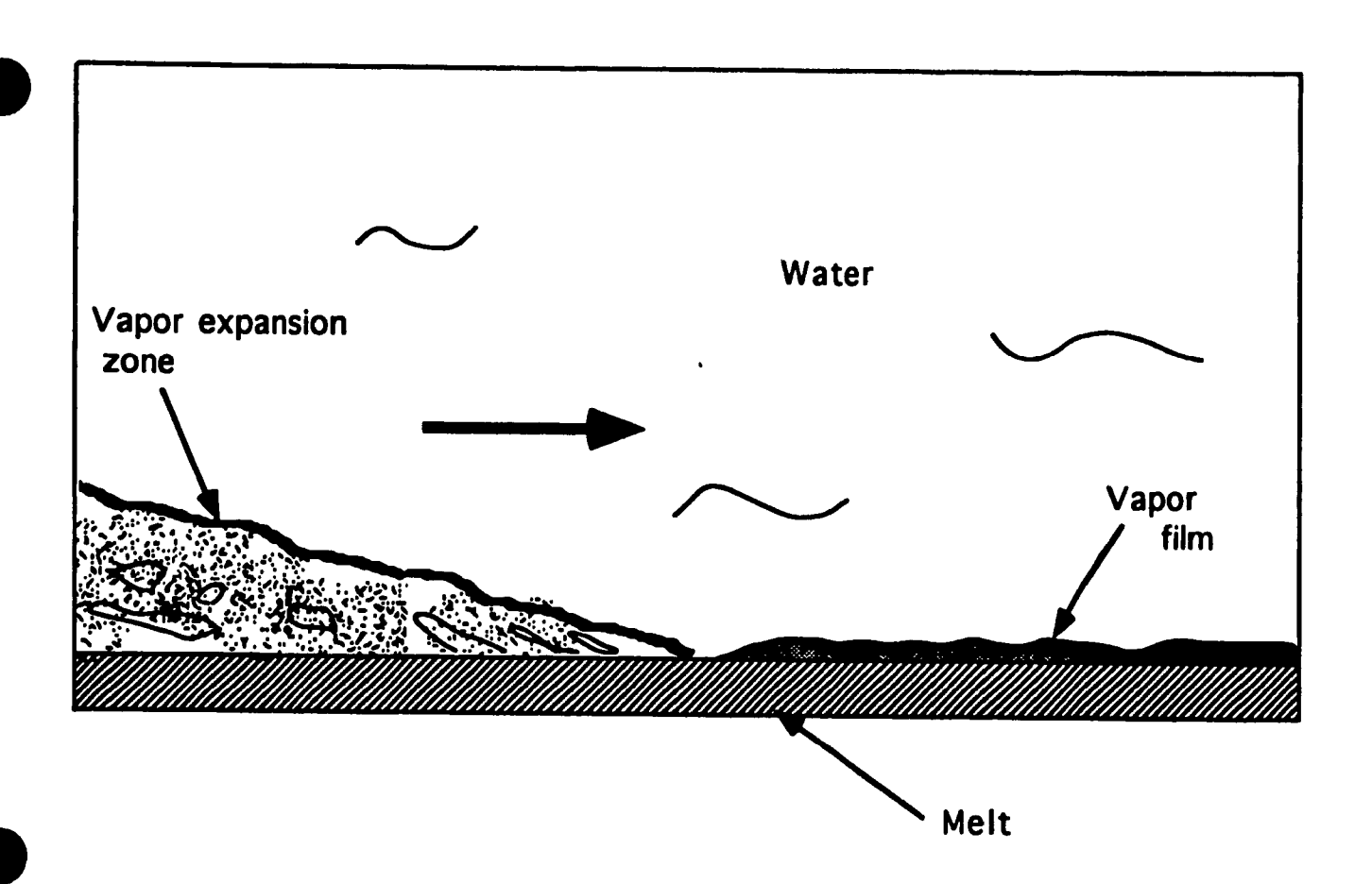


Fig.17 Schematic of vapor explosion propagation.

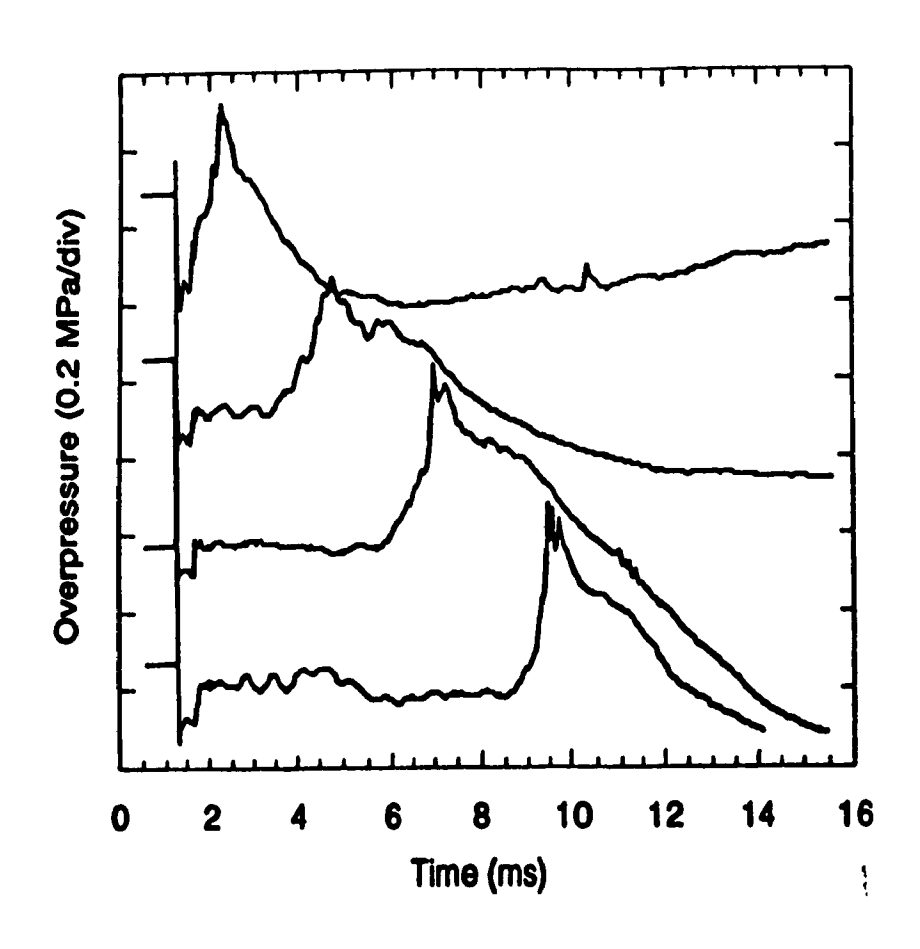


Fig.18 Pressure recorded during propagating interaction in narrow channel. Space between transducers is 10.2 cm. (Ciccarelli et al.)

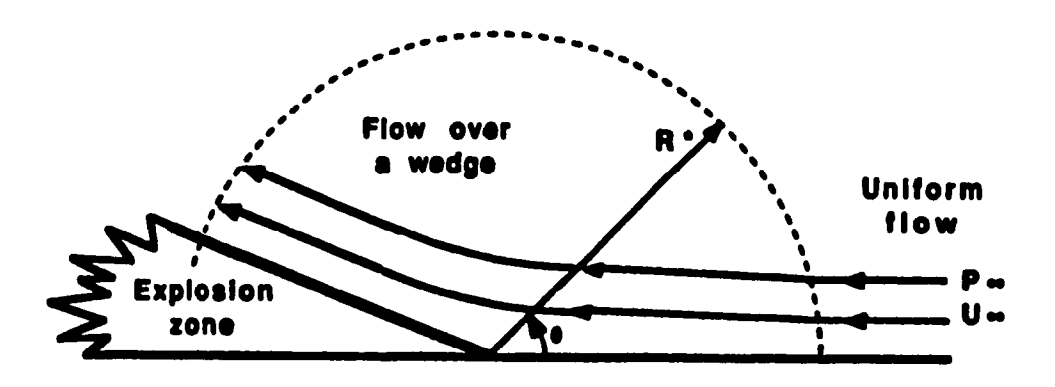


Fig. 19 Schematic of potential flow model for flow of water above explosion zone. (Ciccarelli et al., 1991)

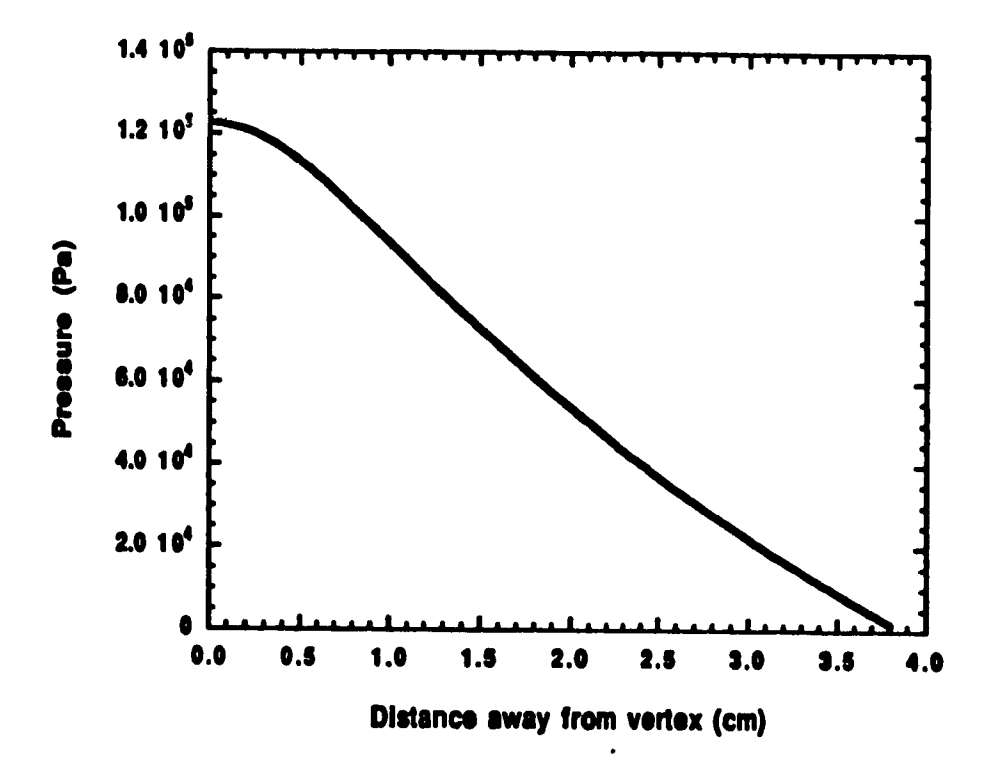


Fig.20 Pressure variation in water from potential flow model of wedge.

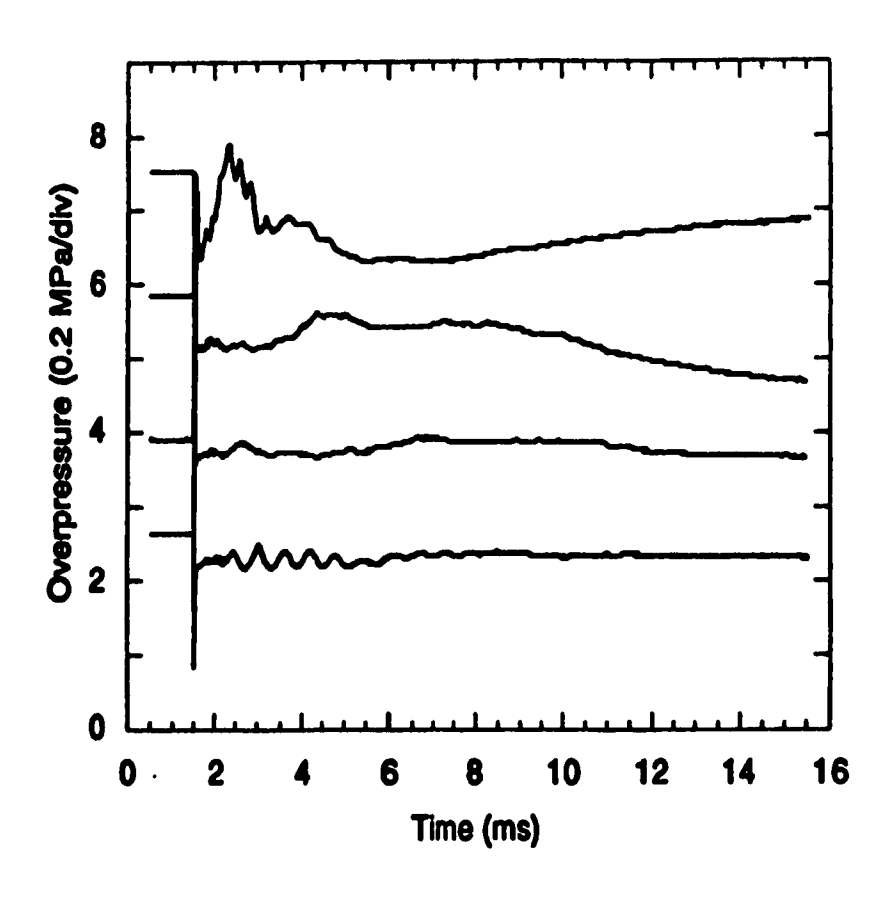


Fig.21 Pressure record illustrating failure of propagation in narrow channel for a water height of 5 cm. (Ciccarelli et al., 1991)

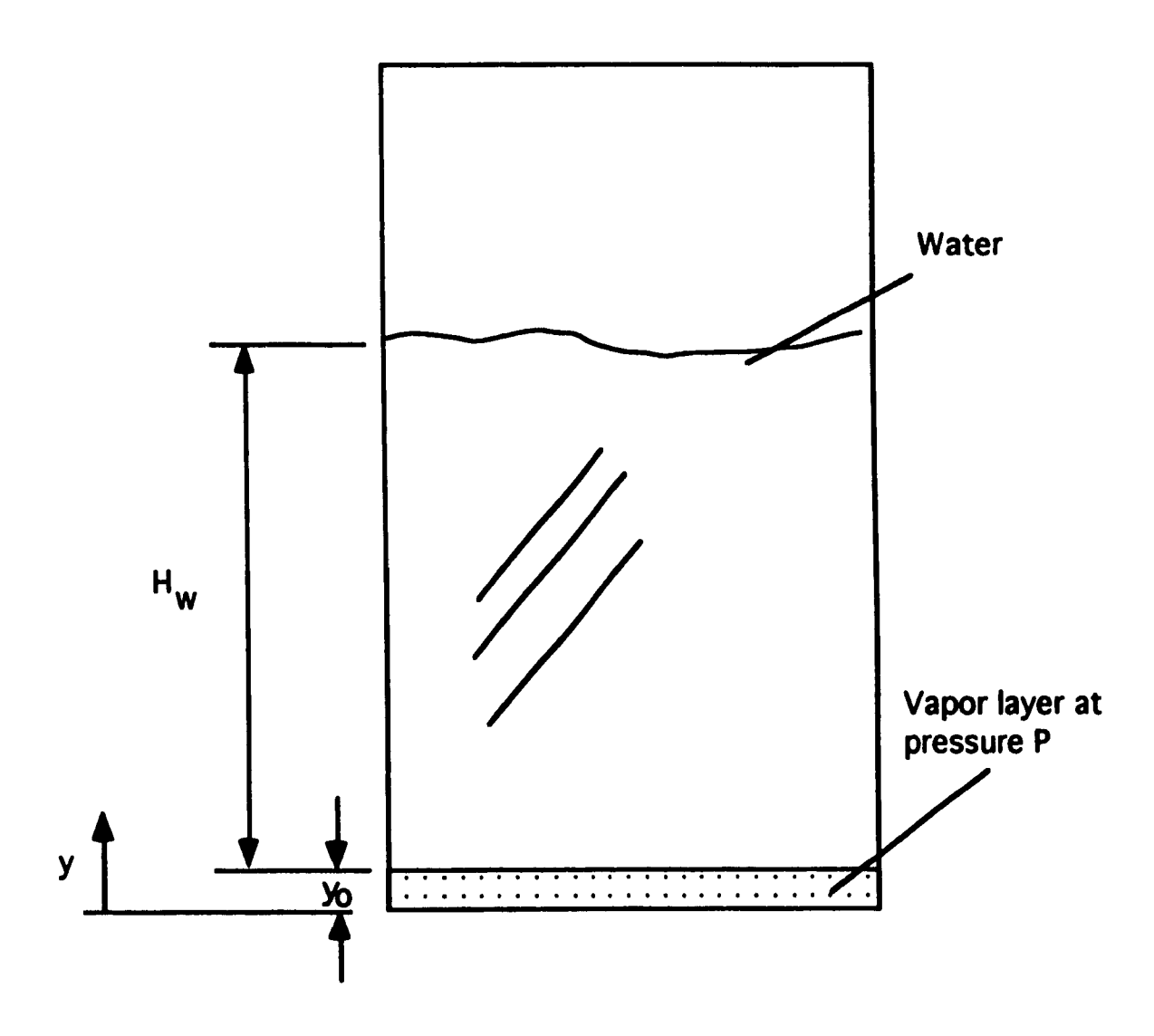


Fig.22 Schematic of one-dimensional expansion of thin vapor layer under water column.

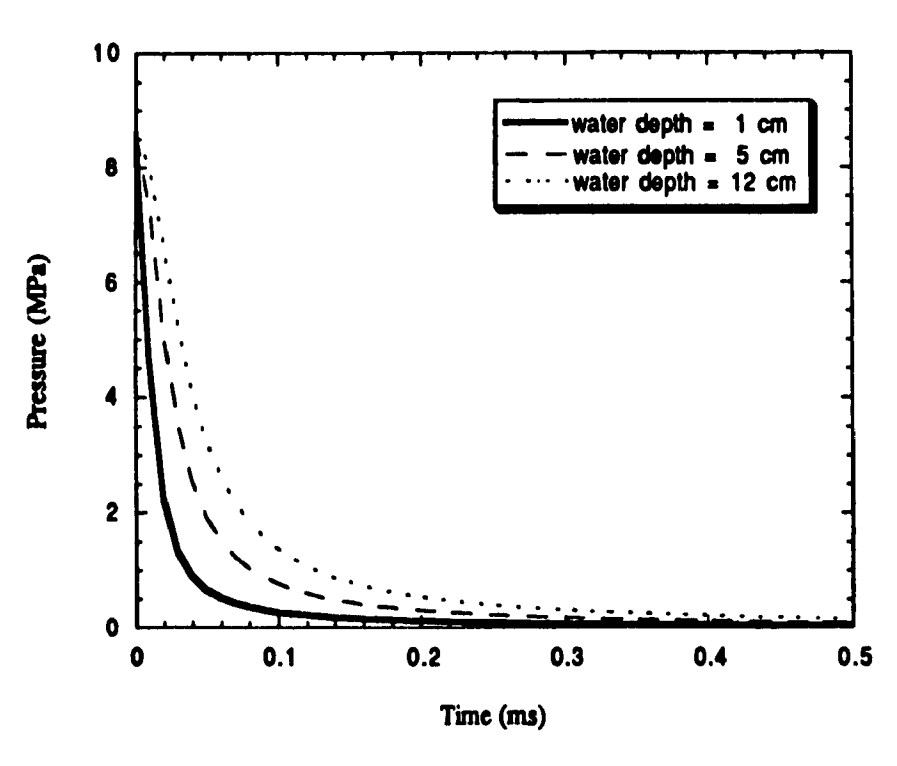


Fig.23 Effect of water height on pressure decay of onedimensional vapor layer below column of water.

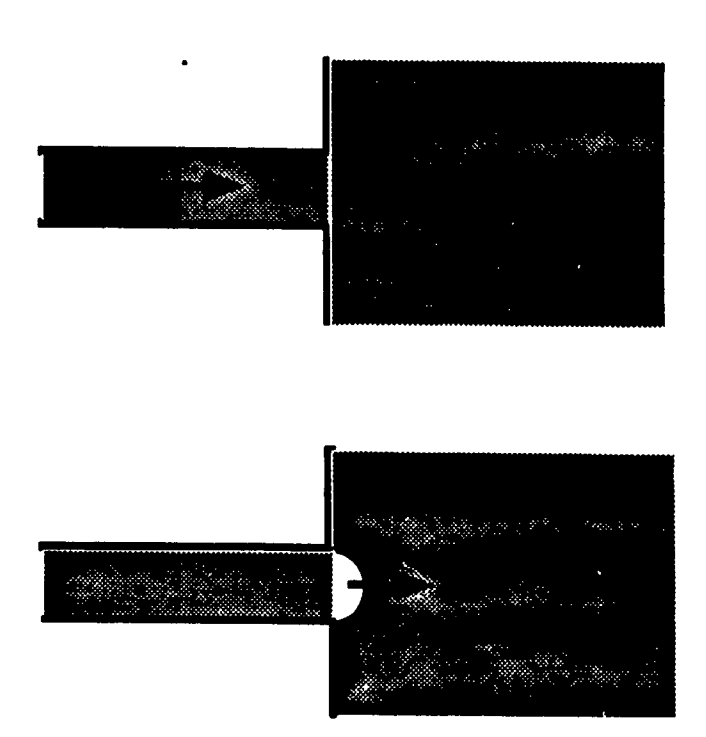


Fig.24 Schematic of propagating interaction subjected to a sudden change in confinement, creating curvature of the interaction front.

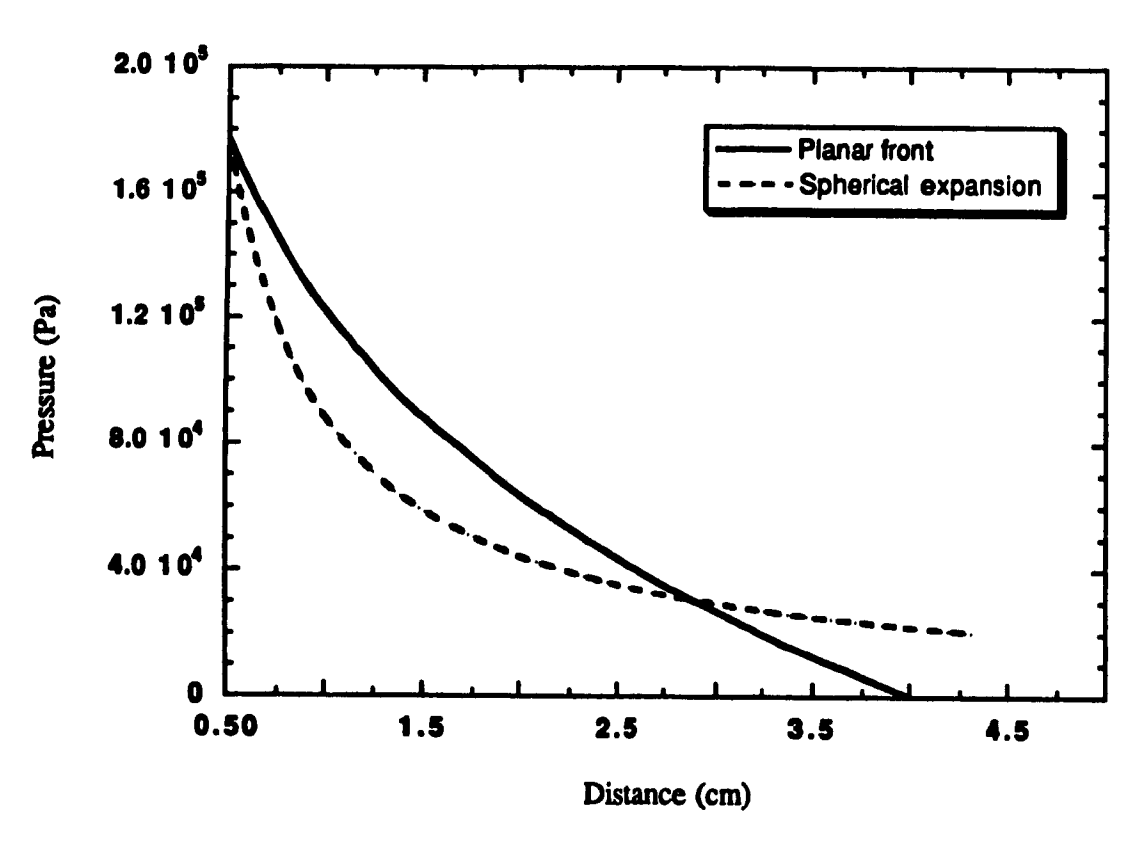


Fig.25 Comparison of pressure decay ahead of planar and spherical interaction front.

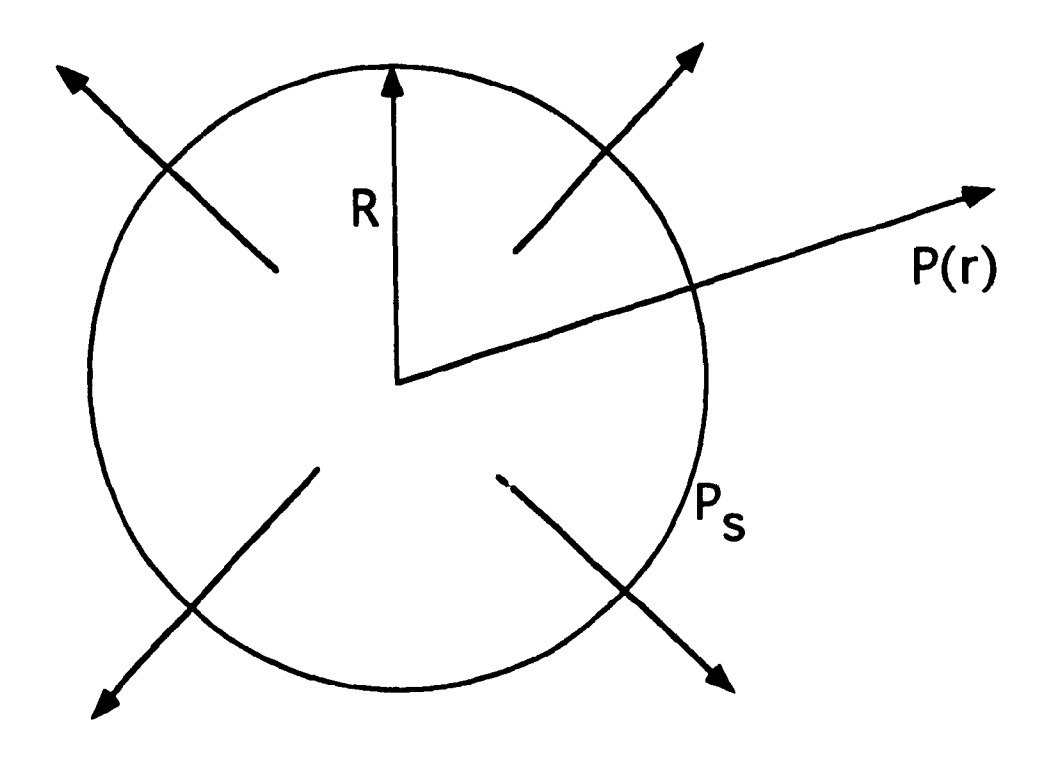


Fig.26 Schematic of cylindrical potential flow model.

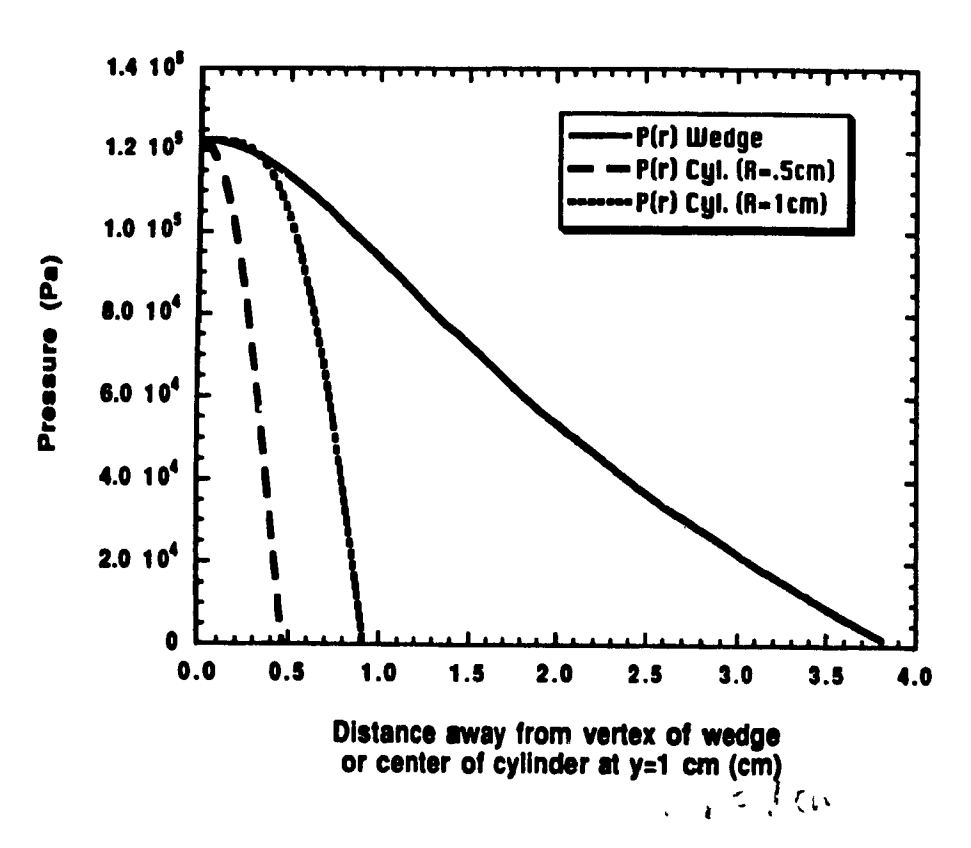


Fig.27 Comparison of pressure variation in water from potential flow models of wedge and expanding cylinder.

Table 2 Effect of geometry on interaction energetics.

Geometry	Yield/Surface Area for Single Interaction (J/cm ²)	Effective Mixing Depth for Single Interaction* (mm)
Single Drop (.5 g)	.55	-
Narrow Channel	.31 [†]	2.0
Cylindrical Tank	.30 §	.86

^{*}definition of mixing depth corresponds to the fraction of the mass of tin fragmented to particle sizes less than 1 mm †estimated from the kinetic energy imparted to the water slug above the tin layer §estimated by integrating the pressure profiles recorded

REFERENCES

- R.P. Anderson and D.R. Armstrong, Laboratory Tests of Molten Fuel-Coolant Interactions, *Trans. Am Nucl. Soc.*, Vol. 15, pp. 313-314 (1972).
- R. Anderson, D. Armstrong, D. Cho and A. Kras, Experimental and Analytical Study of Vapor Explosions in Stratified Geometries, ANS Proc. of the 1988 National Heat Transfer Conf., 3, pp. 236-243 (1988).
- K.H. Bang and M.L. Corradini, Stratified Vapor Explosion Experiments, ANS Proc. of the 1988 National Heat Transfer Conf., 3, pp. 228-235 (1988).
- K.H. Bang and M.L. Corradini, Vapor Explosions in a Stratified Geometry, Nucl. Sci. and Eng., 108, pp. 88-108 (1991)
- S.G. Bankoff, Destabilization of Film Boiling, *Physico Chemical Hydrodynamics*, Vol.1, pp. 69-76 (1980).
- G.K. Batchelor, An Introduction to Fluid Mechanics, Cambridge University Press, Cambridge, UK (1967)
- K.J. Baumeister and F.F. Simon, Leidenfrost Temperature Its Correlation for Liquid Metals, Cryogens, Hydrocarbons and Water, *Transactions of the ASME*, Vol. 95(2), pp. 166-173 (1973).
- T.A. Bjornord, An Experimental Investigation of Accoustic Cavitation as a Fragmentation Mechanism of Molten Tin Droplet in Water, MIT-C00-2831-3TR (1974)
- T.A. Bjornard, W.M., Rohensow and N.E. Todreas, The Pressure Behavior Accompaning the Fragmentation Of Tin in Water, *Trans. Am. Nuc. Soc.*, Vol.19, pp.249 249 (1974)
- S.J. Board, R.W. Hall, and R.S. Hall, Detonation of Fuel Coolant Explosions, *Nature*, Vol. 254, pp. 319-321 (1975).
- S.J. Board and R.W. Hall, Propagation of Thermal Explosions: 1 Tin/Water Experiments, CFRSWP/PP(74)11, CEGB Rept. RD/B/N2850, Central Electricity Generating Board, Berkely Nuclear Laboratories, Berkely, Gloucestershire, UK., (1974).
- S.J. Board and R. W. Hall Recent Advances in Understanding Large-Scale Vapor Explosions, Proc. Thira Specialist Meeting on Sodium Fuel Interactions in Fast Reactors, Tokyo, L. pan, March (1976).
- A.J. Briggs, Experimental Studies of Thermal Interactions at AEE Winfrith, *Proc. of Third Specialist Meeting on Sodium Fuel Interactions in Fast Reactors*, Tokyo, Japan, March (1976).
- D.J. Buchanan and T.A. Dullforce, Mechanism for Vapor Explosions, *Nature*, Vol. 245 (1973)

- L.D. Buxton and W.B. Benedick, Steam Explosion Efficiency Studies; part I SAND79-1399, NUGEG/CR-0947, Sandia National Laboratories (1979)
- L.D. Buxton and L.S. Nelson, Steam Explosions, Chap. 6 of Core-Meltdown Experimental Review, Sandia National Labs. Rept. SAND74-0382 (1975).
- G. Ciccarelli, D.L. Frost and C. Zarafontis, Dynamics of Explosive Interactions Between Molten Tin and Water in Stratified Geometry, *Prog. in Astronautics and Aeronautics*, 134, AIAA, Washington, pp. 307-325 (1991).
- G. Ciccarelli, Investigation of Vapor Explosions with Single Molten Metal Dropsin Water Using Flash X-Ray, *Ph.D Thesis*, McGill University, Mech. Eng. Dept, Montreal, Quebec, Canada (1992)
- S.A. Colgate and T. Sigurgeirsson, Dynamic Mixing of Water and Lava, *Nature*, Vol. 244, pp. 552-555 (1973).
- M.L. Corradini, B.J. Kim and M.D. Oh, Vapor Explosions in Light Water Reactors: A Review of Theory and Modelling, *Progress in Nuclear Energy*, Vol. 22(1) (1988).
- M.L. Corradini, W.M. Rohsenow, and N.E. Todreas, A Proposed Model for Tin-Water Interactions, Paper presented at ASME Winter Annual Meeting, San Francisco, Ca., pp. 17-28 (1978).
- A.W. Cronenberg and R. Benz, Vapor Explosion Phenomena with Respect to Nuclear Reactor Safety Assessment, Adv. in Nucl. Sc. and Tech, Vol. 12 (May 1980)
- D.S. Drumheller, The Initiation of Melt Fragmentation in Fuel-Coolant Interactions, *Nuclear Science and Engineering*: 72, p 347-356 (1979).
- T.A. Dullforce, D.J. Buchanan, and R.S. Peckover, Self-Triggering of Small-Scale Fuel Coolant Interactions: I Experiments, J. Phys. D.: Appl. Phys. 9, pp. 1295-1303 (1976).
- T. Enger amd D.E. Hartman, Explosive Boiling of Liquified Gases in Water, Nat. Res. Council Conf. on LNG Importation and Terminal Safety, Boston, Mass, (1972).
- H.K. Fauske, On the Mechanism of Uranium Dioxide-Sodium Explosive Interactions, *Nuclear Science and Engineering*: 51, p. 95-101 (1973).
- H.K. Fauske, Some Aspects of Liquid/Liquid Heat Transfer and Explosive Boiling, *Proc. of Fast Reactor Safety Meeting*, Beverly Hills, Ca. (April 1974).
- D.F. Fletcher and R.P. Anderson, A Review of Pressure-Induced Propagation Models of the Vapor Explosion Process, CLM-P879 (1990).
- G. Frohlich and M Anderle, Experiments for Studying the Initiation Mechanisms for Steam Explosions, Institute fur Kernenergetik und Energiesysteme report IKE2-51, Universität Stuttgart, Stuttgart, FX (1980).

- F.H. Harlow and H.W. Ruppel, Propagation of a Liquid-Liquid Explosion, Los Alamos National Lab., Rept. LA 8971 MS, (1981).
- E.P. Hicks and D.C. Menzies, Theoretical Studies on the Fast Reactors in Maximum Accident, *Proc. Conf. Safety, Fuels, and Core Design in Large Fast Power Reactors*. pp. 654, ANL-7120, Argonne National Lab. (1965).
- G. Long, Explosions of Molten Aluminum in Water Cause and Prevention, *Metal Progress*: 71(5), pp. 107-112 (1957).
- M.J. Moran and H.N. Shapiro, Fundamentals of Engineering Thermodynamics (2nd ed.), Wiley & Sons Inc. (1988).
- E. Nakanish and R.C. Reid, Liquid Natural Gas-Water Reactions, *Chem. Eng. Prog.*, Vol. 67., No. 12, pp. 36-41 (1971).
- P. Naylor, An Experimental Investigation of Untriggered Film Boiling Collapse, AEEW R 1928, UKAEA Winfrith, Dorset (1985)
- P. Naylor, An Experimental Investigation of Triggered Film Boiling Collapse, AEEW R 1929, UKAEA Winfrith, Dorset (1985)
- L.S. Nelson and P.M. Duda, Steam Explosion Experiments With Single Drops of Iron Dioxide Melted With a CO₂ Laser, *High Temperatures-High Pressures*, Vol. 14, pp. 259-281 (1982).
- M. Ochiai and S.G. Bankoff, Liquid-Liquid Contact in Vapor Explosions, *Proc. ANS/ENS Gas Reactor Safety Mtg.*, Chicago, (1976)
- R.C. Reid, Rapid Phase Transitions from Liquid to Vapor, Adv. Chem. Eng. 12, pp. 105-208 (1983).
- J. Sainson, M. Gabillard and T. Williams, Propagation of Vapor Explosions in Stratified Geometry Experiments with Liquid Nitrogen and Water, Specialists Meeting on Fuel-Coolant Interactions, Santa-Barbara, California, USA (1993)
- P.G. Simpkins and E.L. Bales, Water-Drop Response to Sudden Acceleration, *J. of Fluid Mech.*, Vol. 55, p.629 (1972).
- Sir G. Taylor, The Instability of Liquid Surfaces When Accelerated in a Direction Perpendicular to Their Planes, *Proc. Royal Soc.*, Ser. A, Vol. 201, p. 192 (1950).
- F.M. White, Fluid Mechanics (2nd ed.), McGraw Hill, U.S.A. (1986)
- L.C. Witte, J.E. Cox, and J.E. Bouvier, The Vapor Explosion, J. of Metals, Vol. 22, No. 2, pp. 39-44 (1970).
- W. Zyskowsky, Study of the Thermal Explosion Phenomenon in Molten Copper-Water System, Int. J. Heat and Mass Transfer, Vol. 19, pp. 849-868 (1976).

APPENDIX A

A.1 Hydrodynamic fragmentation models

Boundary layer stripping

Taylor (1965) first proposed a boundary layer stripping model for a drop in a coolant flow. By virtue of the shear forces exerted on the upwind drop surface its surface layer is set into motion, convecting a boundary layer of mass to the equator. At this point the inertia of the layer surpasses the drop surface tension forces causing mass to be stripped away.

Wave crest stripping

This means of mass stripping arises from the growth of waves on the upwind drop surface due to interface instability. The upwind drop surface is subjected to drag forces which induce an acceleration. Since the acceleration is directed from the lighter liquid (coolant) to the heavier one (melt), surface perturbations will tend to grow in the manner of Rayleigh-Taylor instabilities. Also the relative flow between the drop and the coolant is a source of Kevin-Helmholtz instabilities on the drop surface. As the instability waves grow in amplitude they are convected towards the drop equator by the coolant flow. This flow erodes the wave crests producing mist of fine droplets which follow the flow. Further, when the wave amplitudes reach some fraction of the perturbation wavelength they break off from the drop surface before passing the equator.

Catastrophic break-up

The flow of the coolant over the drop creates a pressure difference over its surface, the pressure being higher at the stagnation point than at the drop equator. This pressure difference causes a flattening of the drop perpendicular to the flow. In addition, the coolant flow over the drop surface gives rise to Rayleigh-Taylor instabilities. When these amplitudes grow to the size of the flattened drop they pierce the drop breaking it up

into much smaller ones. These in turn continue to be eroded through wave crest stripping.

A.2 Thermal fragmentation models

Symmetric film collapse

Drumheller (1979) presented a fragmentation model based on the coolant impact on a drop in film boiling. The impact is due to the passage of a shock wave which causes the symmetric collapse of the vapor film around the drop. The vapor film is compressed and condenses at the interface, producing a condensation wave which moves inward to the drop surface as all of the vapor is condensed. Following this wave is the cold liquid which impacts against the drop surface. This impact generates a shock wave within the drop which converges at the drop center, generating a reflected shock wave which travels radially outward. The associated pressure gradients drive the material in the center of the drop outward. The pressure drops sharply at the center, falling to zero, resulting in extensive fragmentation of the drop.

Splash theory model

The splash model of Ochiai and Bankoff (1976) is a self-mixing theory for the initiation and early propagation of vapor explosions. In this model random local contact between the melt and coolant occur due to capillary instabilities of the vapor film. The contact above the spontaneous nucleation temperature produces vapor bubbles which coalesce into a high pressure layer at the drop surface. This local high pressure exerts an impulse on the drop surface, producing an annular jet of melt directed towards the vapor/coolant interface. The subsequent impact of the annular jet on the coolant induces further melt/coolant contact, resulting in an escalation of the interaction.

Coolant jetting model

A number of fragmentation models have considered that the fragmentation of a melt drop can be achieved through the entrapment and rapid vaporization of coolant within the melt. Buchanan (1973) proposed such a model based on coolant jet penetration into the melt. Initially, a vapor bubble exists on the drop surface and collapses asymmetrically. This collapse forms a jet of coolant which impacts against the drop surface, and if sufficiently strong, penetrates the drop surface. The coolant jet mixes with the melt causing the contact surface area to increase exponentially based on a vortex ring formation mechanism. If nucleation sites are available, the coolant is heated to its saturation temperature and evaporates. In the absence of nucleation sites, the jet is continually heated to its homogeneous temperature. In both cases a vapor bubble forms within the drop and expands causing the fragmentation of the drop in that area. At its maximum expansion the vapor bubble collapses re-initiating the process. Thus the fragmentation of the drop is accomplished through a cyclical vapor bubble growth and collapse process.

Entrapment model

The liquid entrapment model was suggested by Long (1957). It is especially applicable to large scale interactions where molten material is poured into a tank, landing on the base. It is proposed that the coolant may become entrapped between the melt and the tank base. The coolant can then be superheated rapidly and boil explosively, generating a pressure wave which fragments the melt.

Shrinking shell model

In contrast to the models previously described, Zyszkowski's (1976) shrinking shell model suggests that the molten material fragments due to solidification effects. During solidification, it is proposed that the thermal stresses induced are greater than the yield stress of the drop. As the drop shell shrinks, the internal pressure increases ejecting molten material through cracks and fissures on the solid surface. Heat is then transferred through these small jets to the cold liquid, resulting in the cooling of the drop core. With large enough heat transfer rates, a vapor explosion may occur. However, in most vapor

explosion conditions, the interface temperature between the melt and coolant exceeds the freezing point of the melt, therefore ruling this out as a possible mechanism.

A recent comprehensive investigation of the fragmentation mechanism of a molten drop in water was performed by Ciccarelli (Ph.D, 1992), using X-ray and high speed photography. The radiographs showed that, during the first vapor bubble expansion surrounding a molten tin drop, fine filaments of metal are ejected from the drop surface and break up into small fragments which are dispersed in the vapor phase medium. Upon the collapse of this vapor bubble, the surface of the drop is highly convoluted, resulting in a second, more energetic vapor bubble expansion due to the enhanced surface area available for heat transfer.

APPENDIX B

Question of fragmentation

A key aspect of the detonation model is whether the inherent fragmentation process is adequate to sustain the shock wave. More precisely, does the necessary fragmentation take place over a sufficiently short time scale so that the energy released goes into supporting the front. The fragmentation mechanisms integrated into the detonation models are almost all based on differential velocity break up, considering boundary layer stripping, Rayleigh-Taylor instability or a combination of both.

Board and Hall (1975) used the data of Simpkin and Bales (1972) on the break-up of liquid drops behind a shock front. The correlation predicts that a drop of diameter D, density ρ_d , in a flow velocity U and density ρ_c , breaks up in a time t_b as given by the following dimensionless time T^* :

$$T^* = \sqrt{\frac{\rho_c}{\rho_d}} \frac{U t_b}{D} = 22 Bo^{-1/4}$$
 (B.1)

where the Bond number, Bo, is given by

Bo =
$$\frac{\rho_d \ g \ D^2}{\sigma} = \frac{3}{8} \ C_d \ We = \frac{3 \ U^2 \ D \ C_d}{8 \ \sigma}$$
 (B.2)

where C_d is the effective drag coefficient (taken as ~2), s is the surface tension of the drop and a is the acceleration. For the energy release to be efficient in sustaining the shock wave, it must be completed before the velocity of the coolant and fuel droplets equalize. For a constant rate of acceleration, the time for the velocities to equilibrate is given by

$$t_{eq} = \frac{U}{g} \tag{B.3}$$

The acceleration, g, is induced by the coolant flow and can be evaluated by considering a single fuel droplet in a flow of coolant at a velocity U:

$$g = \frac{C_d \pi (D/2)^2 (1/2) \rho_c U^2}{4/3 \pi (D/2)^3 \rho_d} = \frac{3 C_d \rho_c U^2}{4 D \rho_d}$$
(B.4)

Substituting (B.4) into (B.3) gives

$$t_{eq} = \frac{3 \rho_d D}{4 \rho_c U C_d}$$
 (B.5)

The condition then for an efficient energy release is that $t_b < t_{eq}$. For tin droplets 1 cm in diameter in water this condition is satisfied for Bo > 10^4 . Board and Hall (1975) calculated the CJ condition of the tin/water system, yielding a Bond number of 10^5 directly behind the shock front. Since this value is greater than 10^4 they concluded that a thermal detonation is possible with fuel fragmentation induced by Rayleigh-Taylor instability.

The correlation of Simpkin and Bales (1972) implemented in Board and Hall's (1975) model is based on the break-up of liquid drops in air. Such data was initially used by vapor explosion workers however it was later recognized that the drop break-up in a liquid/liquid system could be fundamentally different. Patel and Theofanous (1981) studied the fragmentation of mercury, gallium and acetylene tetra bromide drops in water. Their results suggested that the break-up was much faster than observed in previous experiments, giving the following correlation for the dimensionless break-up time:

$$T^* = 1.66 \text{ Bo}^{-1/4} \cong .4$$
 (B.6)

Their work therefore also confirmed that the fragmentation was sufficiently rapid to support a detonation. However subsequent work (e.g. Baines and Butley,1979) revealed longer break-up times in the order of 4.0, closer to those of gas/liquid systems. Such discrepancies have been attributed to a degree of arbitrariness as to the definition of the break-up time.